# Nonlinear seismic response of mid-rise Modular Buildings subjected to near-field ground motions

Amirhossein Emamikoupaei [a©], Ali Bigdeli [b©], Konstantinos Daniel Tsavdaridis[c*]

[a] *Department of Civil and Environmental Engineering, Shahid Beheshti University, Tehran, Iran*

[b] *Department of Civil and Environmental Engineering, Tarbiat Modares University, Tehran, Iran*

[c]*Department of Engineering, School of Science & Technology, City, University of London, Northampton Square, EC1V 0HB, London, UK*

[*]*Corresponding author:* konstantinos.tsavdariidis@city.ac.uk

© *These authors contributed equally to this work.*

## Abstract

In recent earthquakes, structures near seismic sources have suffered severe damage due to near-fault ground motions. When compared with ordinary ground motions, these ground motions create high demands on structures. The presence of a strong energy pulse has been observed in near-fault ground motions. This impulsive motion, propagating towards the site, will result in forward-directivity effects. This study is intended to assess the structural effects of mid-rise Modular Steel Building (MSBs) under the near-fault pulse-like and non-pulse-like records and to investigate design procedures that explicitly comprise near-fault effects. The main objective of this paper is the nonlinear seismic responses of MSBs to near-fault forward-directivity (FD) and non-forward-directivity (NFD) ground motions, as well as whether the equivalent pulse present in forward-directivity earthquake ground motions dominate the structural response. This paper discusses the key properties that can be used to characterize near-fault ground motions with forward-directivity effects and non-forward-directivity effects on the engineering demand parameters. For this purpose, using 72 pulse-like ground motions and 120 non-pulse-like ground motions, a Cloud analysis is conducted to obtain statistically significant results. Nonlinear time history analysis is performed using OpenSees based on distributed plasticity approach to develop a finite-element model of a 6-story mid-rise MSB. The results depict that near-field pulse-type ground motions generate larger demands to the MSB compared with the non-pulse ground motions. In addition, when correlated with simple intensity measures such as PGA, PGV, and spectral acceleration at the first mode period, the structural response to forward-directivity ground motions exhibits a higher dispersion than the structural response to non-forward-directivity ground motions. The representative equivalent pulses of the considered forward-directivity ground motions were decomposed using the continuous wavelet transform method to explore their effects on the MSB response. Finally, the influence of the pulse parameters, including period and amplitude of the forward-directivity, are ascertained.

***Keywords:*** Modular Steel Buildings; Inter-connection; Near-fault ground motions; Forward-directivity; Distributed plasticity; Equivalent pulses

## 1. Introduction

In contrast to traditional on-site construction, modular construction is a fast-evolving method. Modular units as well as their interior components such as studs, walls, ceilings, floors, etc., are delivered to the construction site and assembled to form a building [1], [2][3]. The assembly line method of construction in the factory can reduce time, cost, and waste while ensuring a high level of quality control and accuracy throughout the manufacturing process [4], [5][6]. There are limited studies conducted to evaluate the seismic behavior of modular building systems (MBSs), despite their different behaviors to that of traditional on-site buildings [7] [8], mainly due to the several causes, the vast majority of modular buildings are currently low-rise. First, the current modular building design practices are mostly based on codes for conventional structural systems, owing to the lack of design provisions. Secondly, the seismic performance of MBS, especially mid-rise MBS, is not adequately understood, as it is a relatively new structural form. Finally, difficulties can also arise due to transportation restrictions on module sizes/weights and limited lifting capacities of tower cranes [9].

In the study of seismology and earthquake engineering, identifying the features of near-field records and their influence on different types of structures and their seismic performance is a challenging issue. In the vicinity of seismic sources, near-field ground motions have caused considerable damage. In comparison to regular ground movements, near-field ground motions occur in a wide variety and impose a substantial demand on buildings. According to a growing body of research, near-fault ground motions are characterized by a strong energy pulse [10]. The ground motions recorded in the vicinity of active faults (within approximately 20 km) are notably distinct from those of other locations. Both forward and backward rupture directivity recordings are included in the record set. If the rupture propagates toward the site, the recording at the site will demonstrate forward-directivity effects. Since the propagation occurs at a velocity near to the shear wave velocity, the majority of the seismic energy from the rupture arrives at the location as a big motion pulse at the beginning of the record [11]. Due to the limited bandwidth of the velocity pulse, forward-directivity ground motions can be described by similar pulse models [12]–[17]. These pulses have four primary characteristics: (1) pulse time, (2) pulse amplitude, (3) phase parameter, and (4) number of significant pulses [12], [18]. Due to the short distance traveled by seismic waves, near-fault ground motions are also rich in high frequencies, as the high-frequency content is not often damped, as is the case with far-fault earthquake records. In structural analysis, the impacts of pulse-type ground motions should be evaluated due to the characteristics of the forward-directivity pulses that might influence the response of structures [19]–[27].

Consequently, the aforementioned issues compel the examination of the seismic performance of modular steel mid- and high-rise buildings under forward-directivity ground motions and indicate the urgent need to improve seismic design codes in order to limit the potential damage caused by forward-directivity ground motions on these types of structures.

## 2. Background

### *2.1. Modular steel buildings*

The examination of the seismic performance of modular steel buildings has drawn the interest of researchers, especially for system-level investigations[28]. The seismic performance of low-rise modular buildings in resisting lateral earthquake loads has been investigated by many studies. Fiorino et al. [29] investigated the seismic performance of a full-scale two-story sheathing-braced cold-formed steel modular building. The main focus of the research was on the seismic response of the proposed structural solution, in which the lateral force-resisting (seismic resistant) system is based on CFS floors and walls sheathed with gypsum-based panels. The building was designed according to typical European seismic intensity for areas with medium seismic hazard (PGA of 0.25 g). The building was subjected to white-noise tests and earthquake tests. In order to evaluate the global building seismic response, shake table tests on a full-scale two-story building (macro-scale level) were carried out. The results showed that seismic performance of the CFS modular building was improved, resulting in very small maximum and residual inter-story drift ratio. Macillo et al.[30] evaluated the seismic response of cold-formed steel building four full-scale shear walls sheathed with nailed gypsum panels and relevant panel-to-frame connections made with ballistic nails. The experimental results illustrated that the cyclic loads gave a reduction of wall lateral strength of 20%, whereas the variation of the aspect ratio from 1 to 0.5 resulted in an increase of strength of 35%. Fathieh et al.[31] studied seismic performance of a 4-story modular steel building. The research was conducted by two types of analysis; (1) incremental dynamic analysis (IDA) and (2) nonlinear static pushover analysis. Nonlinear static pushover analysis is widely used to determine the ultimate lateral load resistance of the structure. The result showed that the maximum base shear that the structure can resist is relatively high in the MSB structures. Yi Hu et al.[32] investigated the seismic responses and damage evaluation of near-fault ground motions on a 6-story cold-formed steel modular building. The results revealed that near-fault pulse-like records impose higher damage to mid-rise CFS building compared to non-pulse-like ground motions.

*2.2. Buildings*

In a series of studies, Bertero et al. [33] assessed the structural damage caused by the 1971 San Fernando earthquake, which was characterized by a high-amplitude and long-duration pulse in the acceleration and velocity time histories of several near-fault records. The findings demonstrated that such pulses might generally be typical of near-fault motions, and in general, significant ground velocities may be developed at near-fault locations. Vijay Sharma et al. [34] examined the seismic fragility of semi-rigid (SR) steel moment frames under the near-fault earthquakes with four earthquakes, including far-field, near-field, high directivity, and low directivity, and fling-step consisting of ensembles of ten real ground motion records in each ensemble. For the near-field earthquake with directivity impact, the frequency effects on fragility curves were studied by altering the peak ground velocity (PGV) to peak ground acceleration (PGA) ratio with high (> 160 cm/s-g) and low (< 160 cm/s-g) ratios. They concluded that a near-field earthquake's high directivity ratio considerably impacts the risk of exceeding compared to a far-field earthquake. Anderson et al. [19] evaluated the uncertainties of the selection of the design earthquake for a specific building's nonlinear dynamic responses with a 10-story steel frame subjected to the ground motions recorded in the near-fault zone during the 1979 Imperial Valley earthquake. They concluded that the nonlinear response of structures to near-fault ground motion is more sensitive to the pulse duration in comparison to the basic period of the structure. Liao et al. [35] investigated the dynamic response of a 12-story and 5-story reinforced concrete structure with moment-resisting frames under near-fault and far-fault records. Based on their findings, story drifts and base shear for RC moment-resisting frames due to near-fault ground motions were much greater than those caused by far-fault ground motions. It has been shown in an analysis of the correlation between the dynamic response characteristics of structures and parameters of near-fault ground motions, such as the PGV/PGA ratio, spectral velocity, and ground input energy, that maximum story drift increases with increasing values of these factors. Alavi and Krawinkler [25] presented quantitative information about significant response features of elastic and inelastic frame structures exposed to near-fault ground movements with forward-directivity pulses. It was demonstrated that the distribution of story ductility is determined by the base shear strength and the ratio of the structure's fundamental period (T) to the pulse period (Tp), such that within the approximate period range of $0.375 < T/Tp < 3.0$, As a substitute for actual near-fault ground motions, simple equivalent pulses can be used in structural analysis. Sehati et al. [36] investigated the structural response of multi-story structures to near-fault ground motions employing the Incremental Dynamic Analysis and studied whether the structural response is dominated by ground motion pulses present in forward-directivity ground motions. In addition, they studied whether simplified pulses are capable of expressing the structural response consequences of these pulses. When $0.5 < T_{pulse}/T_{structure} < 2.5$, they found that dynamic studies employing an equivalent pulse model provide structural responses comparable to those estimated for forward-directivity pulses. In this period range, the response of the structures was governed by forward-directivity pulses, and the response may be predicted using equivalent pulses. Outside of this range, the forward-directivity pulse could not control the response of the structures. Gerami and Abdollahzadeh [37] studied the influence of forward-directivity on the vulnerability distribution of steel moment-resisting frames with a few number of spans using a nonlinear dynamic analysis of five structural models of varying heights subjected to ground motions near to the fault. They demonstrated that forward-directivity has no substantial influence on the distribution of base shear over the height of the frame. In addition, the results demonstrated that structure height plays a substantial role in amplifying forward directivity effects in the bottom half of low-rise steel moment frames and the lower one-third of high-rise steel moment frames in the vicinity of the fault zone. Taiyari et al. [38] investigated two distinct sets of pulse-like and non-pulse near-field records on the behavior of steel moment-resisting frames (MRFs). It was determined that MRF buildings have superior seismic performance under non-pulse-like ground motions compared to pulse-like ground motions. The average response modification factor derived from non-pulse-like ground motions was around 5, which was 1.19 times more than the values obtained from pulse-like records. The seismic response of steel special moment frames (SMFs) of 3, 5, and 8 stories was examined by Mansouri et al. [39], taking into account the effects of panel zone modeling and forward-directivity near-field ground motions effect. The nonlinear time-history analysis of the model was conducted along with various engineering demands parameters such as floor displacements, inter-story drift ratios, story accelerations, and story shears for steel moment frames. In the presence of a velocity pulse with the forward directivity effect, they revealed that steel moment frame structures required to exhibit exceptional ductility were impacted by substantial displacement demands. Comparing the median maximum drift during near-field records with forward-directivity influence and far-fault earthquakes revealed that the amount of drift was 3.47, 4.86, and 5.92 times greater in 3, 5, and 8-story structures, respectively.

*2.3. Special structures*

Qiang Xu et al. [40] investigated the inherent self-similarity between seismic characteristics and the dynamic behavior of a concrete gravity dam under near-fault ground motions. They found that intensity and pulse parameters play a significant role in the practical seismic design of concrete gravity dams. Yazdani and Alembagheri [41] studied the nonlinear seismic response of gravity dams subjected to forward-directivity (FD) and non-forward-directivity (NFD) earthquake ground motions near the fault. It was demonstrated that the FD records produce more dispersion in the EDPs compared to the NFD records. In addition, the seismic response under the main FD ground motions and their equivalent pulses revealed that the equivalent pulses typically underestimate the EDPs with respect to the FD records. Although several scholars have examined the fragility curves of regular and irregular buildings [42]–[46], the structures of MSBs subjected to near-field ground shakings have been left out.

Although, there is not sufficient information for the seismic design of MSB in near-fault ground motions regions, mid-rise MSB structures may be built in the vicinity of near-fault regions. The aim of the present study is, therefore, to evaluate the seismic responses of MSB subjected to near-field earthquakes and their equivalent pulses. In this way, the most significant concerns regarding the impacts of forward-directivity (FD) and non-forward directivity (NFD) near-fault ground motions on the seismic responses of mid-rise modular steel buildings are examined. First, a description of the database of recorded ground motions is utilized for this investigation and the method is used to extract equivalent pulses from the recorded ground motions. The structural model is then characterized using a methodology based on distributed plasticity and the finite element method. 72 forward-directivity and 122 non-forward-directivity ground motions are utilized to generate statistically meaningful findings. An equivalent pulse model is used [14] so that the equivalent pulses exhibit a similar structural response to the recorded forward-directivity records. Using the OpenSees software, a series of Cloud analyses were conducted to simulate the nonlinear seismic responses under FD near-fault ground motion, equivalent pulses, and NFD near-field ground motions in order to identify an equivalent pulse model that can capture the seismic response of forward directivity earthquake ground motions. The seismic response of the structures to pulse-like ground motions is next investigated.

## 3. **Ground motions and equivalent pulses employed**

In this work, 72 near-field forward-directionality (FD) and 122 near-field non-forward-directivity (NFD) records were employed to assess the seismic response of the modular steel building (MSB) under investigation. The PEER database [47] is used to extract ground motion data. This extended range of ground motions enables the model to display various behaviors, ranging from elastic to failure. Two criteria are used to select non-pulse-like NFD records: (1) fault distance less than 20 kilometers and (2) PGV/PGA ratio larger than 0.1. These FD and NFD earthquake records are based on data from 5<M<9 events and diverse soil types. There are two basic types of ground motions near faults: pulse-like motions and non-pulse-like motions. Pulse-like motions can be classified as "forward-directivity" motions and "fling". Its velocity time history may show the specific nature of the pulse-like motion caused by forward-directionality. Near-fault ground motions have much greater peak ground velocity (PGV) than far-fault ground motions.

(a)

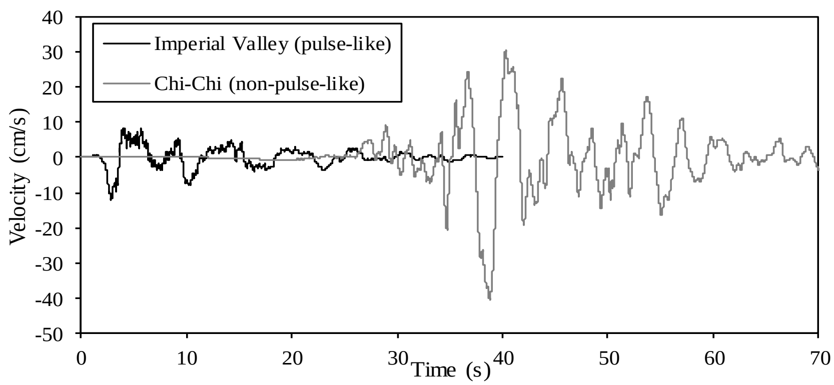

(b)

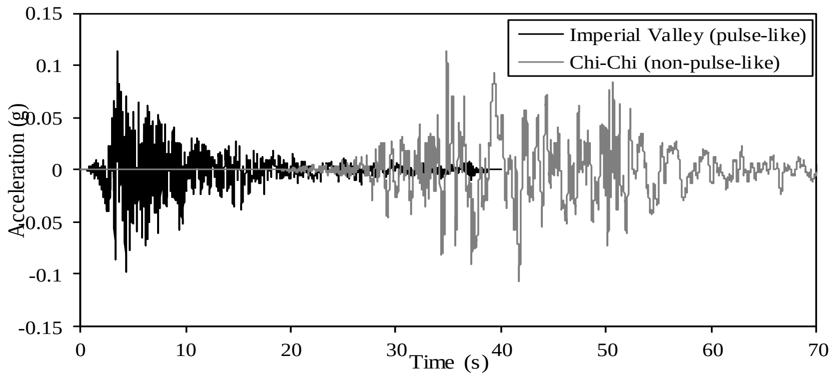


**Figure 1. Comparison of near-fault forward-directivity ground motion and near-fault non-forward-directivity ground motion: (a) velocity; (b) acceleration.**

Figure 1 illuminates ground acceleration and velocity time history of TCU087 ground motion recorded in the Chi-Chi, Taiwan earthquake in 1999 and Westmorland Fire Station ground motion recorded in the Imperial Valley earthquake in 1979. Ground motion Chi-Chi is a typical near-field forward-directivity ground motion, and Imperial Valley is a typical near-field non-forward directivity ground motion. As indicated by the time history of velocity and acceleration, the near-field forward-directivity ground motion contains a large pulse.

A considerable amount of research has been conducted on the development of equivalent pulse models that characterize the special effects of pulse-like motions in order to realize the importance of simple pulse in terms of prediction of seismic response of the structure [36], [48]. Although near-fault ground motions are very complicated, According to recent studies [25], [36], [49], equivalent pulse representations of structures that are subjected to near-fault pulse-like ground motions are capable of capturing the salient response features. To facilitate the investigation of the effects of pulse parameters on the seismic response of structures, equivalent pulse models can be introduced to represent near-fault ground motions. A procedure was developed by Baker [14] for determining the largest velocity pulse within a ground motion. Using a wavelet transform, the dominant pulse is identified, and the wavelet that best matches its frequency and amplitude is extracted from the ground motion. The size of the extracted pulse relative to the original ground motion was also used by Baker as a criterion for classifying a ground motion as pulse-like. The Daubechies wavelet of order 4 was selected as the mother wavelet in the analyses [14]. The following two additional criteria regarding the velocity pulse were applied in order to identify pulse-like records that are possibly caused by directivity effects: (I) it arrives at the beginning of the strong ground motion, and (II) its absolute amplitude is large relative to the remainder of the data. Wavelets can be extracted from ground motion which best corresponds to the dominant pulse and then their amplitudes and pseudo-periods are used to determine the amplitudes and periods of the equivalent velocity pulses. The acceleration response spectra of all chosen recordings are displayed in Figure 2**Error! Reference source not found.**, together with their mean.

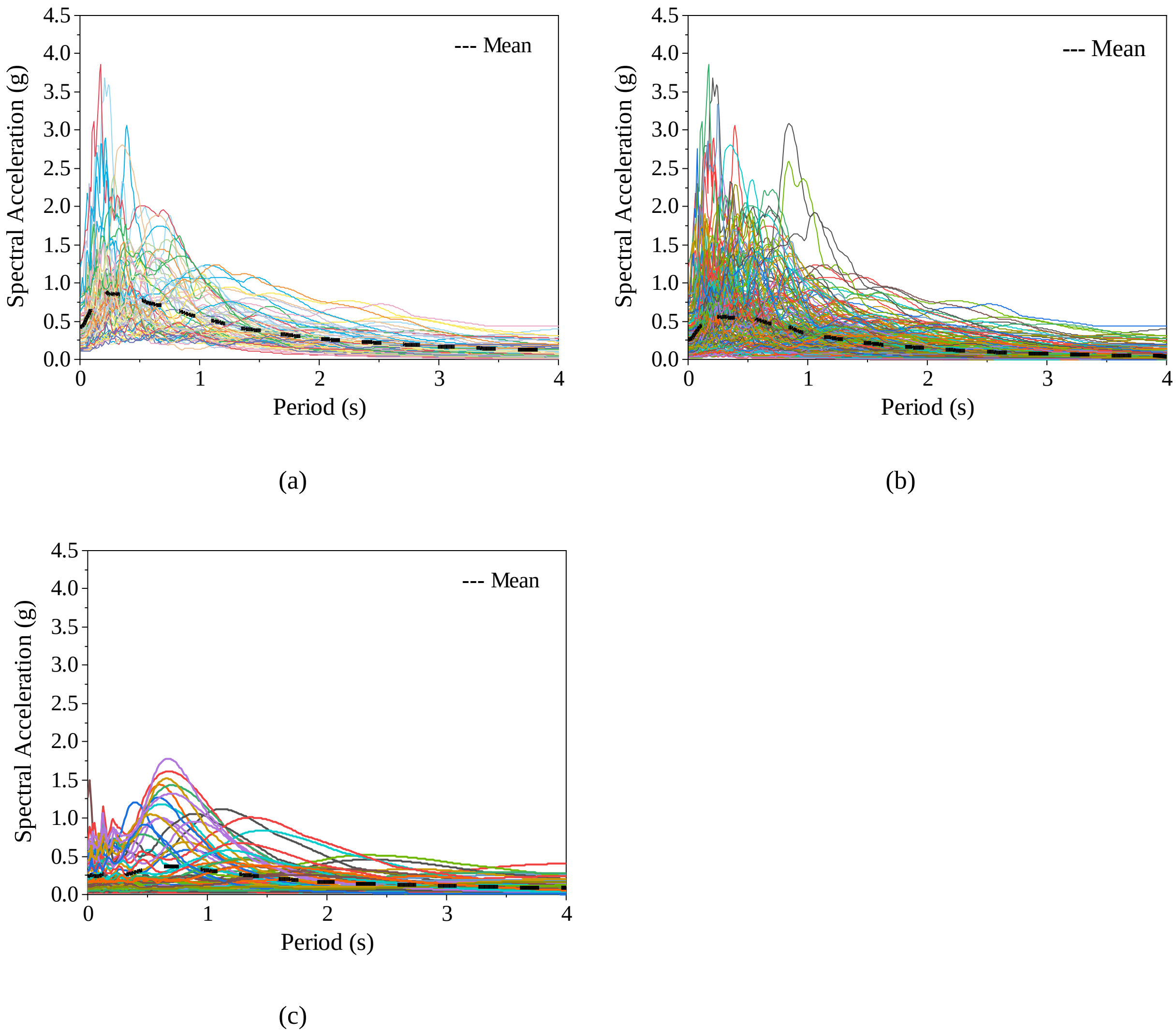


**Figure 2. Acceleration response spectra of all selected ground motions, considering 5% damping for (a) FD records, (b) NFD records, (C) Pulse records**

## 4. MSB numerical model

### *4.1. Model description*

According to AISC[50] [51], a six-story steel MSB braced frame with 25 modules in each story, including five bays in each direction, and a height of three meters per story is utilized to study the effects of forward-direction pulses on mid-rise modular buildings. Each module is six meters long, three meters wide, and three meters high.

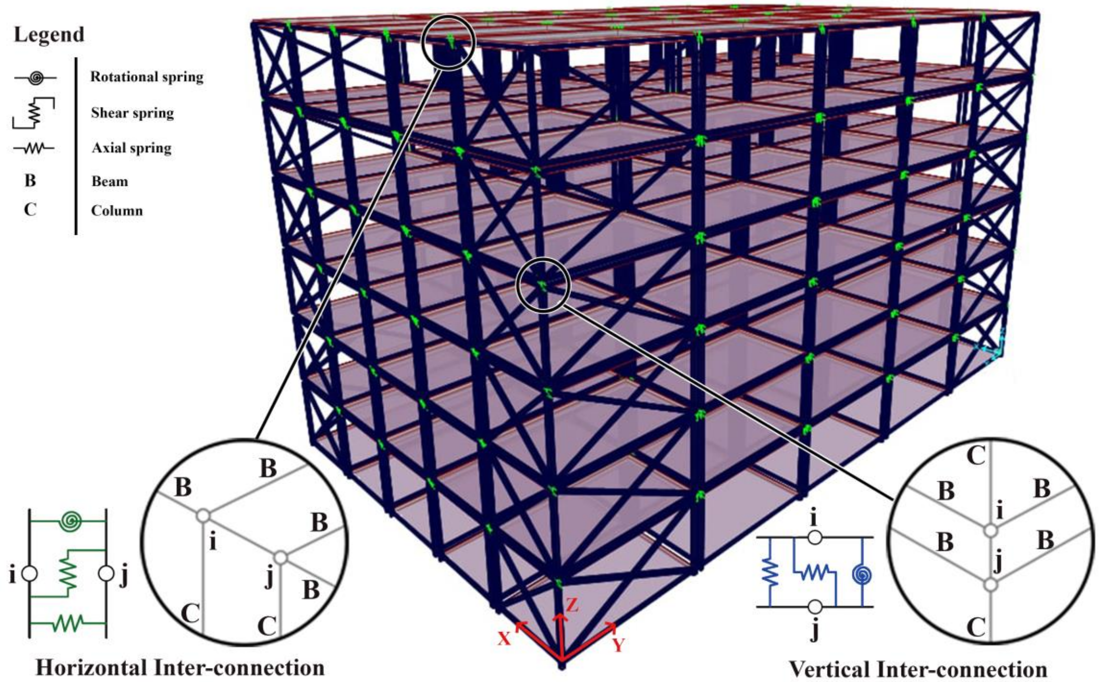


**Figure 3. 3D view of the case study with vertical and horizontal inter-module connection**

A 3D view of the studied MSB is shown in Figure 3 provides details on the optimal frame sections for the MSB's columns, beams, and braces. In MSB constructions, hollow square sections (HSS) are used extensively for columns, beams, and braces. The model accounts for the center-line offset of columns and the small space between consecutive columns by modeling horizontal axis gaps of 350 mm and vertical axis gaps of 200 mm for each module, as shown in Figure 4 (a). Grade 350 steel is used for the steel member, which has a yield strength of 350 MPa and ultimate strength of 450 MPa, with a modulus of elasticity of 200 GPa and a Poisson's ratio of 0.3.

**Table 1 Member section of studied MSB**

| 6-story MSB | | | |
|---|---|---|---|
| Member | Story 1-2 | Story 3-4 | Story 5-6 |
| Column | HSS 152×152×11.8 | HSS 152×152×5.9 | HSS 127×127×5.9 |
| Floor beam | HSS 102×102×5.9 | HSS 102×102×5.9 | HSS 102×102×5.9 |
| Ceiling beam | HSS 76×76×5.9 | HSS 76×76×5.9 | HSS 76×76×5.9 |
| Brace | HSS 127×127×11.8 | HSS 127×127×8.9 | HSS 102×102×5.9 |

*4.2. Nonlinear analysis assumptions*

During this study, only the lateral response of the MSB in the Y direction is considered. It consists of two exterior X-braced frames that are symmetrically located at the corners of the structure's plan to resist lateral forces in this direction. In each story level, the braces are attached to the floor beam-to-column and ceiling beam-to-column joints. Gusset plates are welded to the braces in order to connect the braces to the modular frame system. As shown in Figure 4, a two-dimensional model of the MSB is created using OpenSees software based on the distributed plasticity approach in order to perform a nonlinear dynamic analysis. The nonlinearities of both materials and geometry are taken into account.

The models created to evaluate the seismic response of SCBFs include the nonlinear behavior associated with the yielding of braces in tension, as well as the nonlinear behavior associated with the buckling and post-buckling of the braces. To adjust rotations associated with out-of-plane brace buckling, gusset plates must be designed, which are generally used to connect braces to edging members. The models also took into account the deformation and yielding of gusset plates as well as any yielding in the beams and columns in the connection regions.

The uniaxial material Steel02 option in OpenSees defines the stress-strain relationship of this material. The element *forceBeamColumn* option in OpenSees is used to represent beam and column elements with fiber sections and five integration points per element. Brace elements are Steel02, a uniaxial material in OpenSees, which defines the stress-strain relationship. Elements with fiber sections and five integration points are represented using the forceBeamColumn option in OpenSees. The dispBeamColumn option can also be used to model brace elements, in which fiber sections are included, as well as three integration points for each element. In the analysis, the P-delta effect has been considered as a source of geometric nonlinearity. As a means of discretizing braces, eight elements between work points are used, with each element having three integration points and an initial out-of-plan imperfection of L/500 for each element. Single and multiple springs aligned with the brace and located at the ends were considered in order to adequately capture the out-of-plane rotational behavior of gusset plates at the connections. To accurately determine the buckling capacity of a brace, it is critical to estimate the stiffness of the gusset plate accurately. This has been demonstrated by Hsiao et al. [52]. For welded connections, nonlinear spring elements with zero length were used in OpenSees, allowing for a simulation of strength and stiffness degradation.

A Rayleigh damping ratio of 5% is assigned to the first and second modes of vibration in the nonlinear dynamic analysis to account for damping. A step-by-step numerical integration method is used to conduct the nonlinear time history analysis in which the parameters $\gamma$ and $\beta$ are assumed to be 0.5 and 0.25, respectively. There may be non-convergence problems when analyzing nonlinear static and dynamic systems. Therefore, a solution algorithm object must be defined in order to ensure that the numerical solution is accurate. In order to solve the nonlinear equations, a sequence of steps is identified. Non-convergent solutions are found using various algorithms.

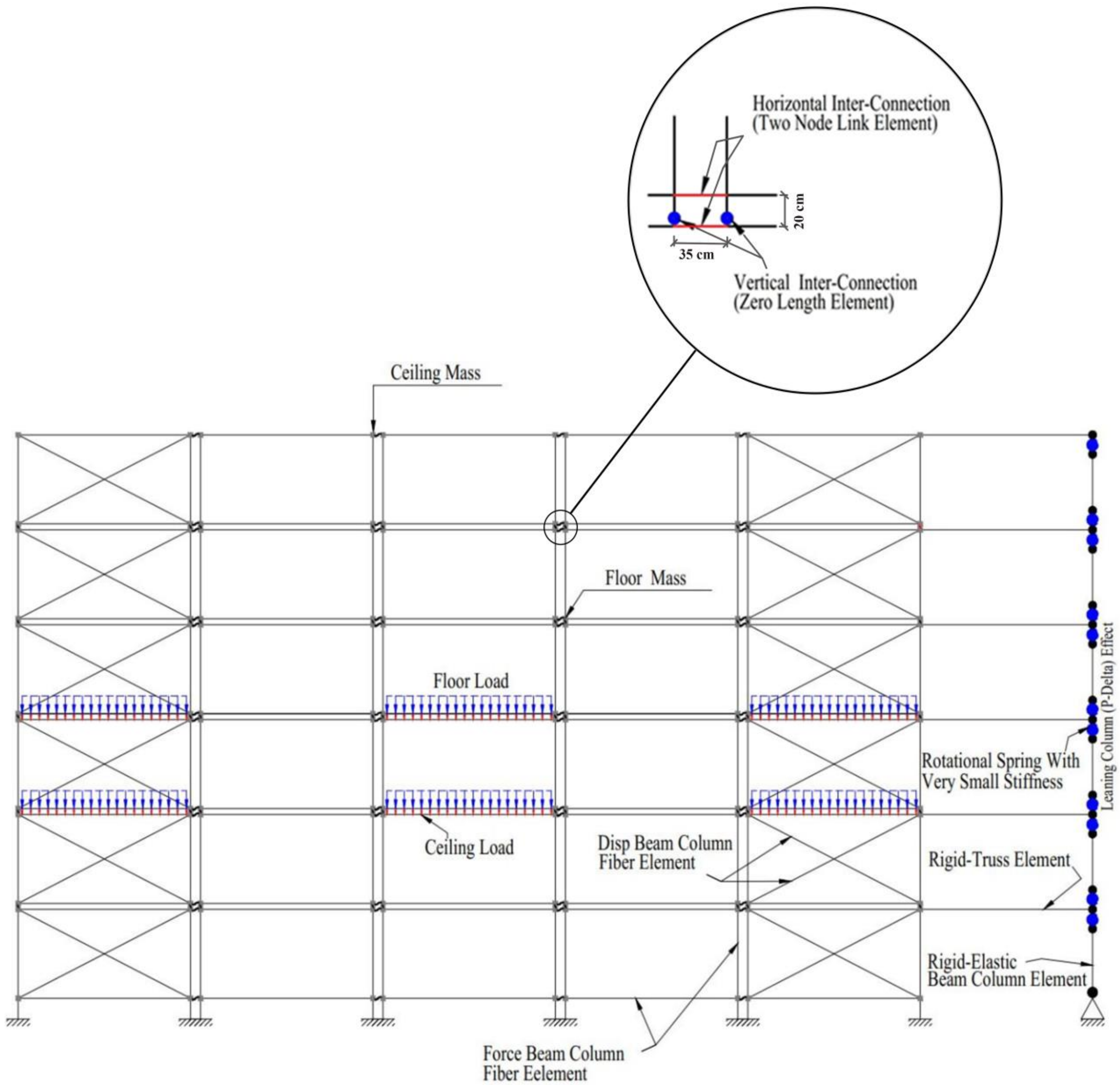

Horizontal Inter-Connection
(Two Node Link Element)
20 cm
35 cm
Vertical Inter-Connection
(Zero Length Element)
Ceiling Mass
Floor Mass
Floor Load
Leaning Column (P-Delta) Effect
Rotational Spring With
Very Small Stiffness
Ceiling Load
Disp Beam Column
Fiber Element
Rigid-Truss Element
Rigid-Elastic
Beam Column Element
Force Beam Column
Fiber Eelement


(a)

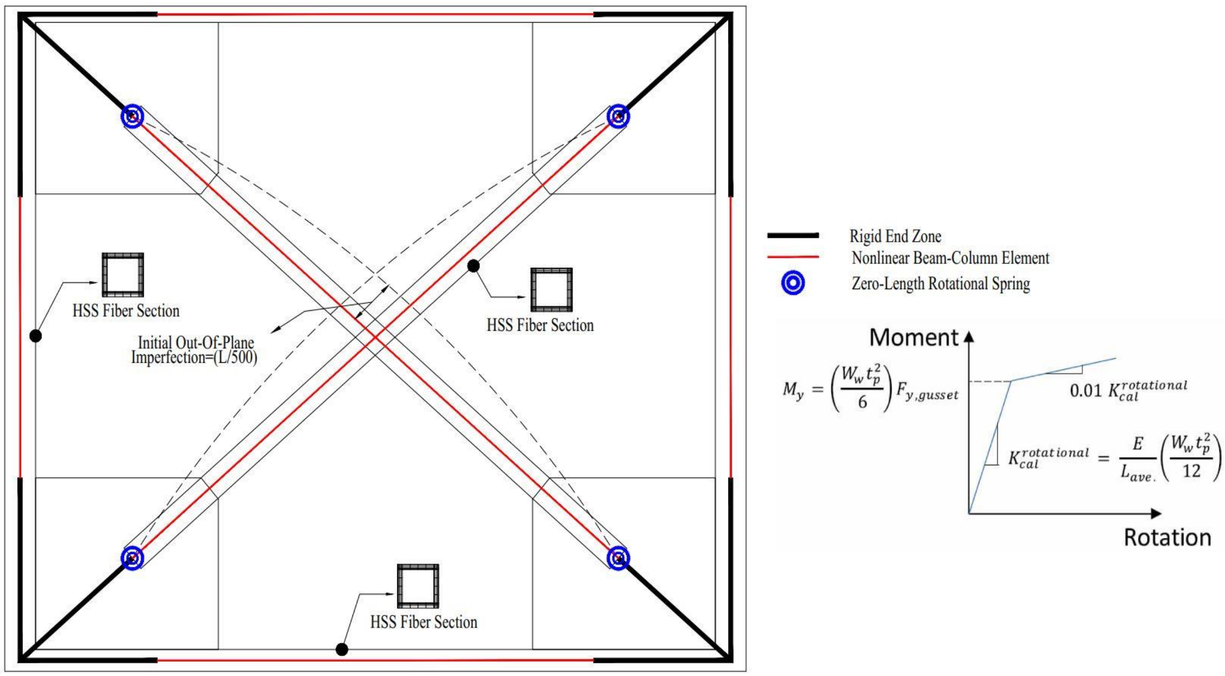


(b)

**Figure 4. Details of modeling the MSB in OpenSees (a) two-dimension model (b) schematic view of brace modeling**

### *4.3. Seismic design assumptions*

The building is designed using ASCE/SEI 7-16 [53]for lateral load loading and AISC 360-16 for steel structure design. In this study, it is assumed that the structure is located near active faults and is designed using seismic design category (SDC) E seismic criteria and evaluated using near-field ground motions. In order to compute the earthquake design force, the following parameters are accounted for: importance factor Ie =1 (Risk Category II for residential buildings), Site Class D (stiff soil), and response modification factor R =6. It is assumed that the structure is located in California. In addition, in order to obtain realistic representation of the braced frame lateral stiffness and better predictions of the building drifts and periods, separated diaphragms (one for each module) were considered at each story floor when modeling a MSB structure.

**Error! Reference source not found.** provides utilized loads such as the floor, roof, corridor, and ceiling, as well as the live loads and the snow load used for the design.

**Table 2. Loads applied for the design of MSB**

| Structural components | Load type | Load |
|---|---|---|
| Floor slab | Superimposed dead load | 0.75 KN/m2 |

| | | |
|---|---|---|
| | Live load | 2 KN/m2 |
| Ceiling slab | Superimposed dead load | 0.7 KN/m2 |
| Roof | Superimposed dead load | 0.32 KN/m2 |
| | Live load | 1 KN/m2 |
| | Snow load | 1 KN/m2 |
| Corridor | Live load | 4.8 KN/m2 |
| External Floor beam | Dead load | 1.5 KN/m |

**Error! Reference source not found.** illustrates the first three in-plane modes of the MSB in Y direction. In the OpenSees model, the MSB is represented as a two-dimensional model in Y-direction. Here, the mode shapes in the Y direction are calculated.

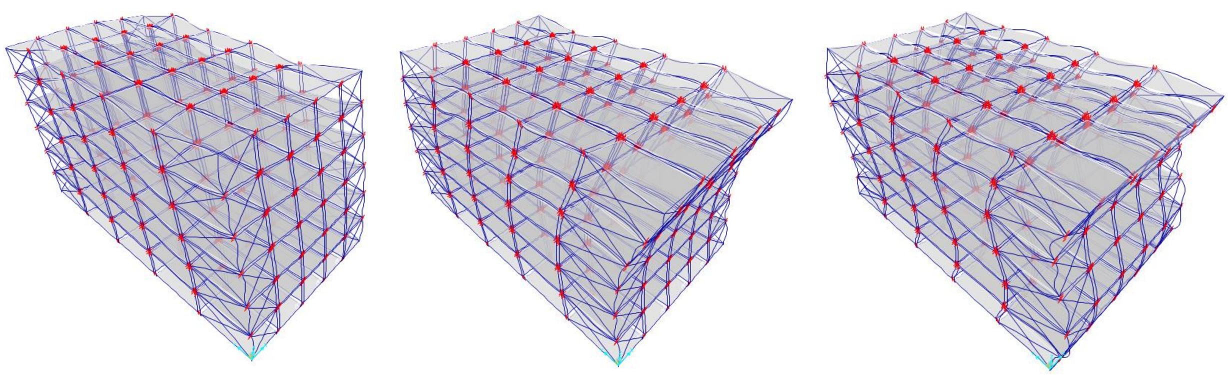

**$f_1$ = 1.191(Hz)** **$f_2$ = 3.571(Hz)** **$f_3$ = 5.556(Hz)**

**Figure 5. 3D-dimensional mode shapes of studied MSB in the Y direction.**

*4.4. Vertical and horizontal inter-connections*

In this study, horizontal and vertical interconnections (HCs and VCs) were modeled in accordance with Styles et al. [54] in order to link modules at their corners. In the case of vertical interconnections, they published force-displacement data. However, no data on moment-rotation was published. Figure 6 (a) to (e) illustrate horizontal and vertical interconnections. Due to the lack of sufficient data available and to simplify the problem, it has been assumed that the moment-rotation behavior of horizontal connections can also be applied to horizontal and vertical connections[28], [55], [56].

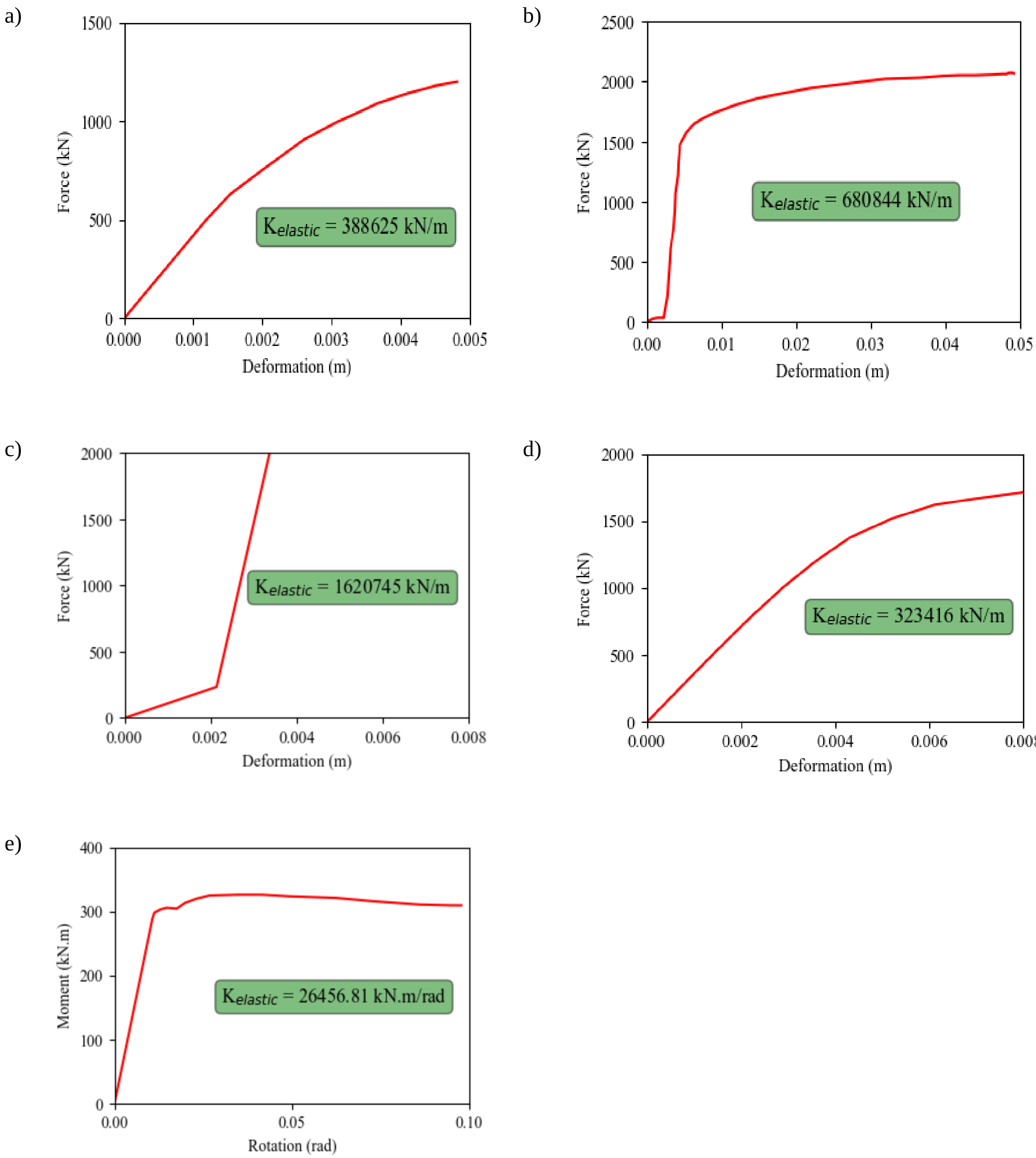


**Figure 6. The Behaviour of (a) HC in the Y direction, (b) HC in the Z direction, (c) VC in the Y direction, (d) VC in the Z direction, (e) HC and VC in the Y and Z directions.**

## 5. Analysis results

Nonlinear seismic analyses were performed for the modular steel building described in the previous paragraph under the FD, the equivalent pulses, and the NFD near-fault ground motions. The engineering demand parameters (EDPs) [57], such as the maximum value of the peak inter-story drift ratio (drift normalized by story height) over all stories is called the Inter-story Drift Ratio (IDR), the maximum value of the peak total drift ratio from base to roof (DR), the Maximum Story Ceiling Displacement (MSCD), the maximum value of the peak ceiling absolute acceleration over all stories of superstructures is known as the Maximum Ceiling Acceleration (MCA), and the Maximum Story Shear (MSS). The maximum inter-story drift ratios of ceiling beam to floor beam (IDR) and maximum story ceiling displacement (MSCD) were selected to describe the seismic behavior of the structure as EDPs.

## 6. Seismic responses under FD and NFD near-fault ground motions

### *6.1 Inter-story Drift Ratio (IDR) responses of MSB*

The IDR response is one of the most significant Engineering Demand Parameters (EDPs) since it is undeviatingly associated with the collapse-resistance performance. The maximum inter-story drift ratios (IDRs) for each story of the 6-story MSB under FD and NFD records are separately illustrated in Figure 7. Also, the maximum coefficient of variation of the IDR for all stories ($\mathrm{CV}_{\mathrm{max}}$) is shown. The coefficient of variation is the ratio of the standard deviation to the mean and shows the extent of variability in relation to the mean. The higher the $C_V$, the greater the dispersion. Since the Cloud Analyses were performed on the MSB, the mean values can better depict the seismic responses for the structure.

Considering the mean values of the IDRs, it can be seen that there is a difference between structural response for the MSB under the FD and NFD records ensembles. The mean values of the structural responses reveal that forward-directivity ground motions impose considerably higher demand to MSB compared to the non-forward-directivity ground motions (Figure 7c). Given the fact that the mean value of the PGAs for FD records is 1.72 times that of NFD records, and their PGVs for FD set is 2.38 times that of NFD set due to the presence of the initial velocity pulse. Meanwhile, the maximum mean values of all IDR demands (Figure 7c) approximately stand at beyond 1% and 0.6% for pulse-like and non-pule-like ground motions, separately. This value for IDR response of MSB undergoing the pulse-like records surpasses the code-specified 1% IDR limit. In addition, Figure 7c shows that under the effect of forward-directivity set and non-forward-directivity set, the IDR demands incline to be concentrated at the intermediate story levels, indicating that the intermediate parts of mid-rise MSBs are more vulnerable to damage than the upper and lower stories for these types of ground motions. Moreover, the dispersion in the structural reactions is larger for the non-forward-directivity set, as shown by the larger value of the maximum coefficient of variation ($CV_{max}$) of IDR, when the structure is subjected to non-forward-directivity ground motions (Figure 7a and b) in comparison with the forward-directivity ground motions. In general, the scattering in the structural response is larger for the non-forward-directivity set compared to the forward-directivity set.

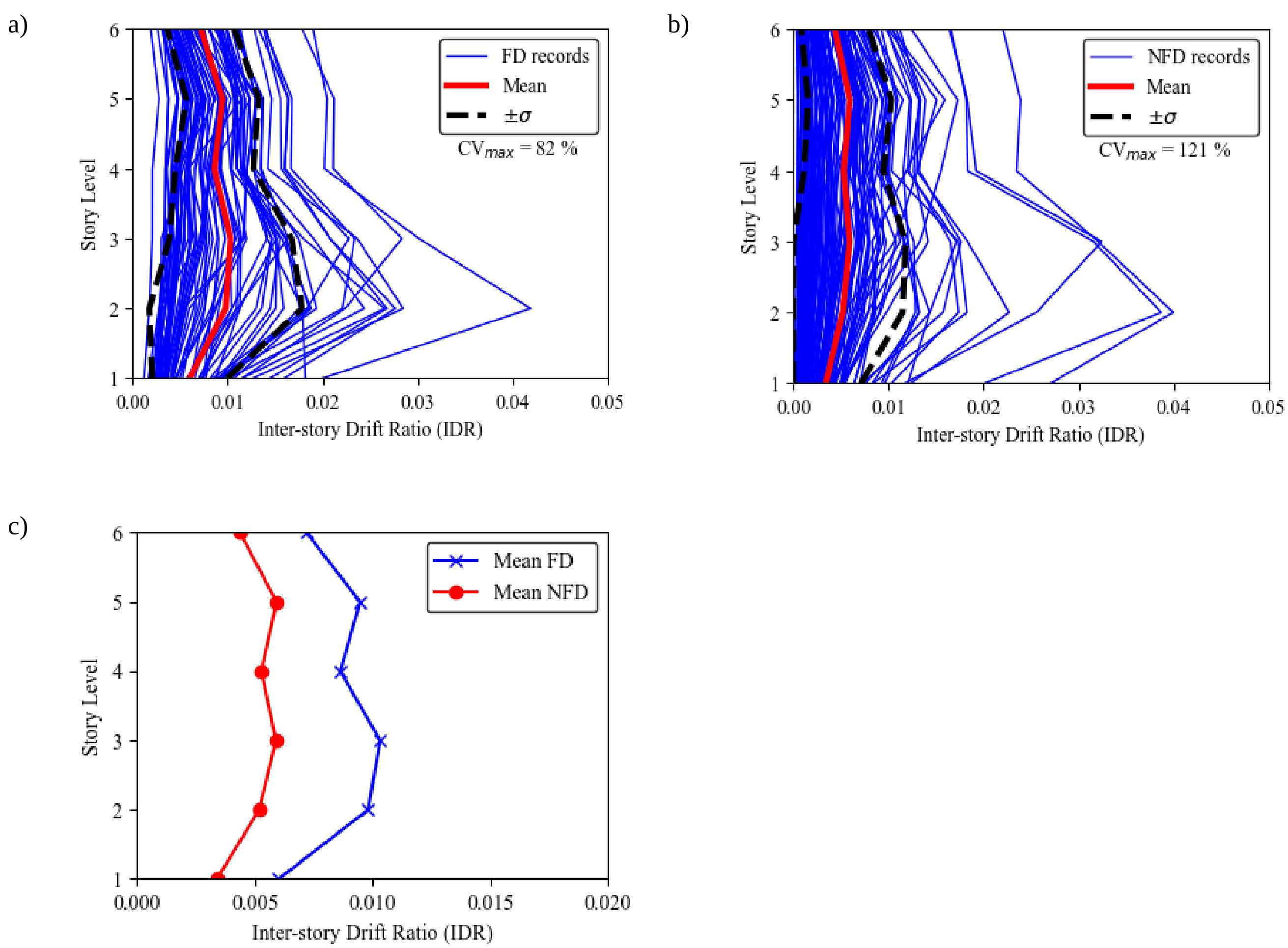


**Figure 7. The inter-story drift ratio (IDR) demand of MSB for a) FD set, b) NFD set, and c) Mean IDR of the FD and NFD sets.**

### *6.2 Maximum Story Ceiling Displacement (MSCD) responses of MSB*

Subsequently, the maximum story ceiling displacement demands and corresponding average values of MSB are shown in Figure 8. Unambiguously, the maximum displacement is augmented along the structure height, and the MSCD demands of MSB reach the largest. This means that the top of the MSB is more prone to damage compared to the lower height. It is also observed from Figure 8c that pulse-like excitations yield more significant damage to MSB with respect to the non-pulse-like ground motions. Due to the fact that the mean value of PGV of forward-directivity ground motions and non-forward-directivity ground motions are 71.23 and 29.92 cm/s, respectively. Therefore, the mean PGV of the FD set is greater, and the corresponding mean MSCD demand of MSB is also greater. To elaborate on the MSCD demands from Figure 8c, when MSB is exposed to forward-directivity ground motions, the maximum displacement response is roughly twice as much as that of non-forward-directivity ground motions standing at nearly 16 cm and 8 cm, separately.

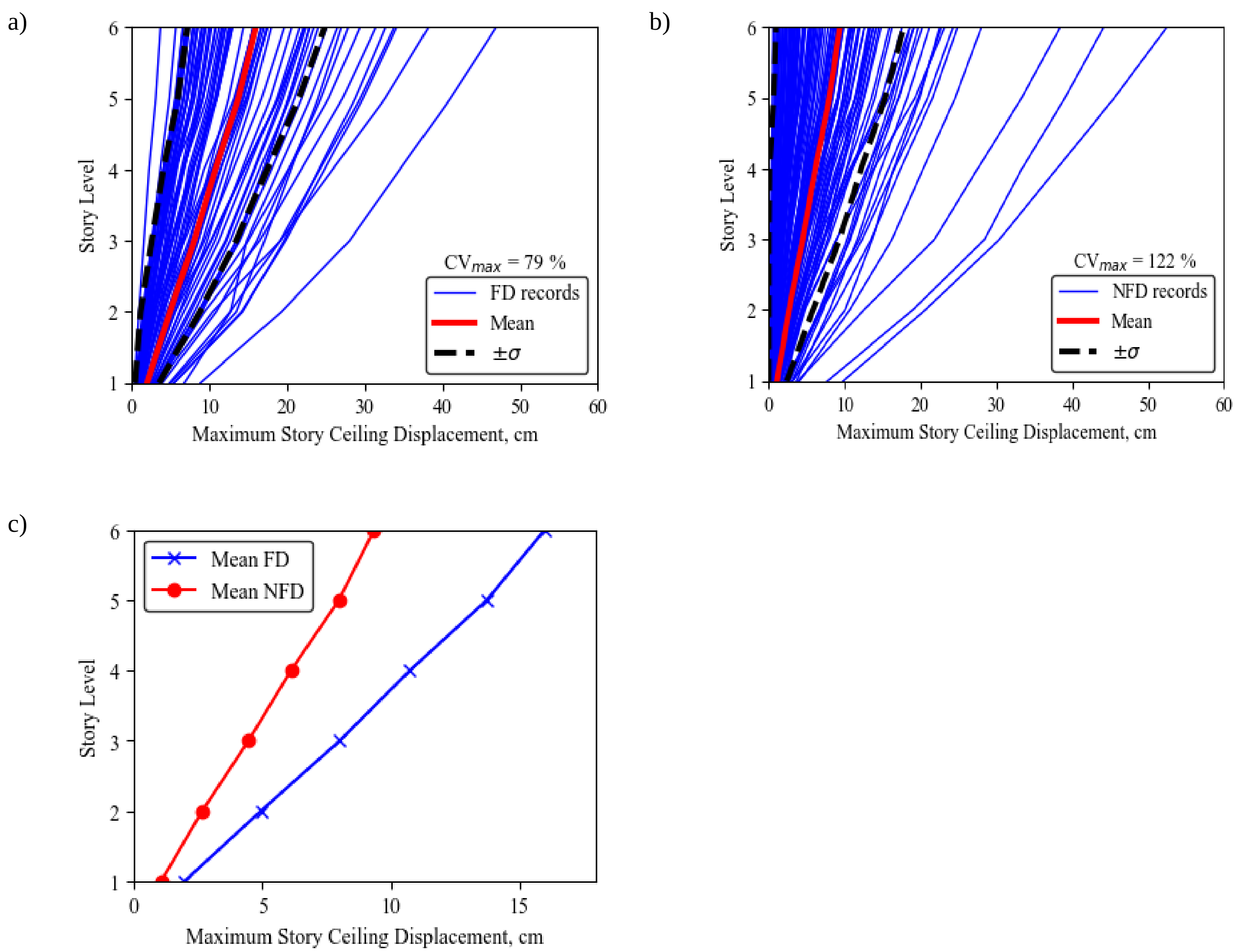


**Figure 8. The Maximum Story Ceiling Displacement (MSCD) demand of MSB for a) FD set, b) NFD set, and c) Mean MSCD of the FD and NFD sets.**

*5.3 Maximum Ceiling Acceleration (MCA) responses for MSB*

In the following, the maximum ceiling acceleration (MCA) responses and the mean values of MSB under FD and NFD ground motions are outlined (Figure 9). The results from Figure 9c reveal that the MCA demands of MSB under both forward-directivity and non-forward-directivity first increase, then decrease and at last increase again and reach a maximum value. Moreover, the mean MCA responses of the structure under the forward-directivity set are highly greater than the non-forward-directivity set. The reason derives from the fact that the mean PGA values for pulse-type and non-pulse-type ground motions are equal to 0.43g and 0.25g, respectively. The results disclose that the mean PGA values of the selected ground motions show a relationship with the MCA demands. In other words, the higher the amount of mean PGA of the ground motions, the greater the amount of MCA demands of MSB. It was also observed that the maximum coefficient of variation of the MCA demands undergoing non-pulse-type ground motions is higher than pulse-type ground motions, specifying that the dispersion of MCA responses under NFD records is considerable.

A)

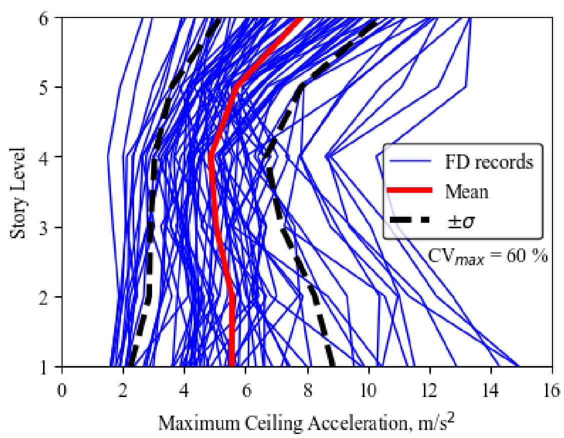


b)

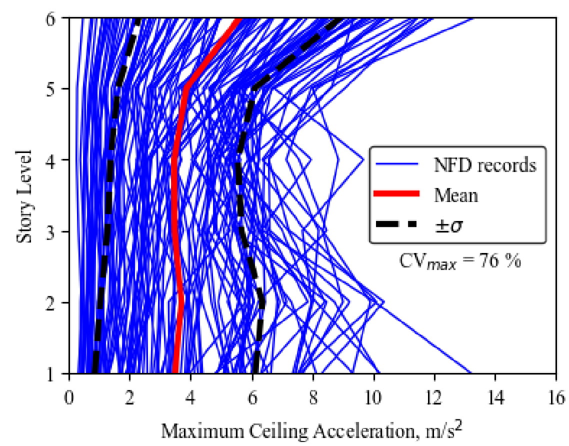

c)

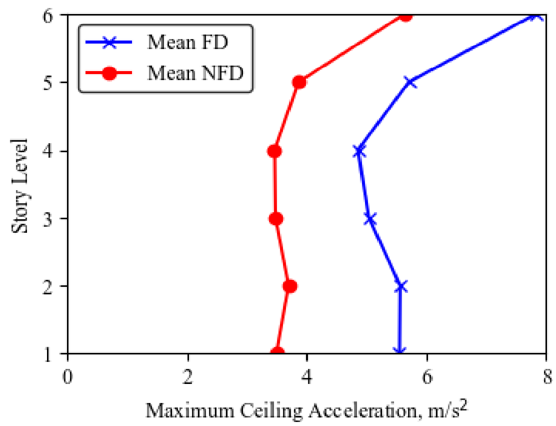


**Figure 9. The Maximum Ceiling Acceleration (MCA) demand of MSB for a) FD set, b) NFD set, and c) Mean MCA of the FD and NFD sets.**

### *5.4 Maximum Story Shear (MSS) responses of MSB*

Maximum Story Shear (MSS) is another seismic Engineering Demand Parameter (EDPs) inspected in this study. Using the algebraic sum of the shear forces between the column and brace elements in each story level, the MSS for that story level was calculated. At first glance, obviously, the maximum values of the mean MSS demand are yielded at the first story level by both earthquake sets (Figure 10). By comparing the results from Figure 10c, it can be derived that the difference between the mean MSS responses of FD and NFD records decreases along the MSB height towards the upper levels. To compare the mean MSS responses of MSB undergoing pulse-type and non-pulse-type ground motions, it is concluded from the Figure 10c that the FD records have caused more damage to structure than that of NFD records. Furthermore, the Figure 10d reveals that the maximum values of MSS responses for MSB subjected to non-pulse-type and pulse-type ground motions are roughly equal excepting the first level, indicating that forward-directivity directly exerts influence on the base shear. This case is originated from the initial velocity pulse of the FD records that affects the structural responses. Notice as well that the dispersion of MSS responses for MSB under NFD records is greater than in NFD records since the NFD set has a larger $CV_{max}$ Figure 10a,Figure ***10***b).

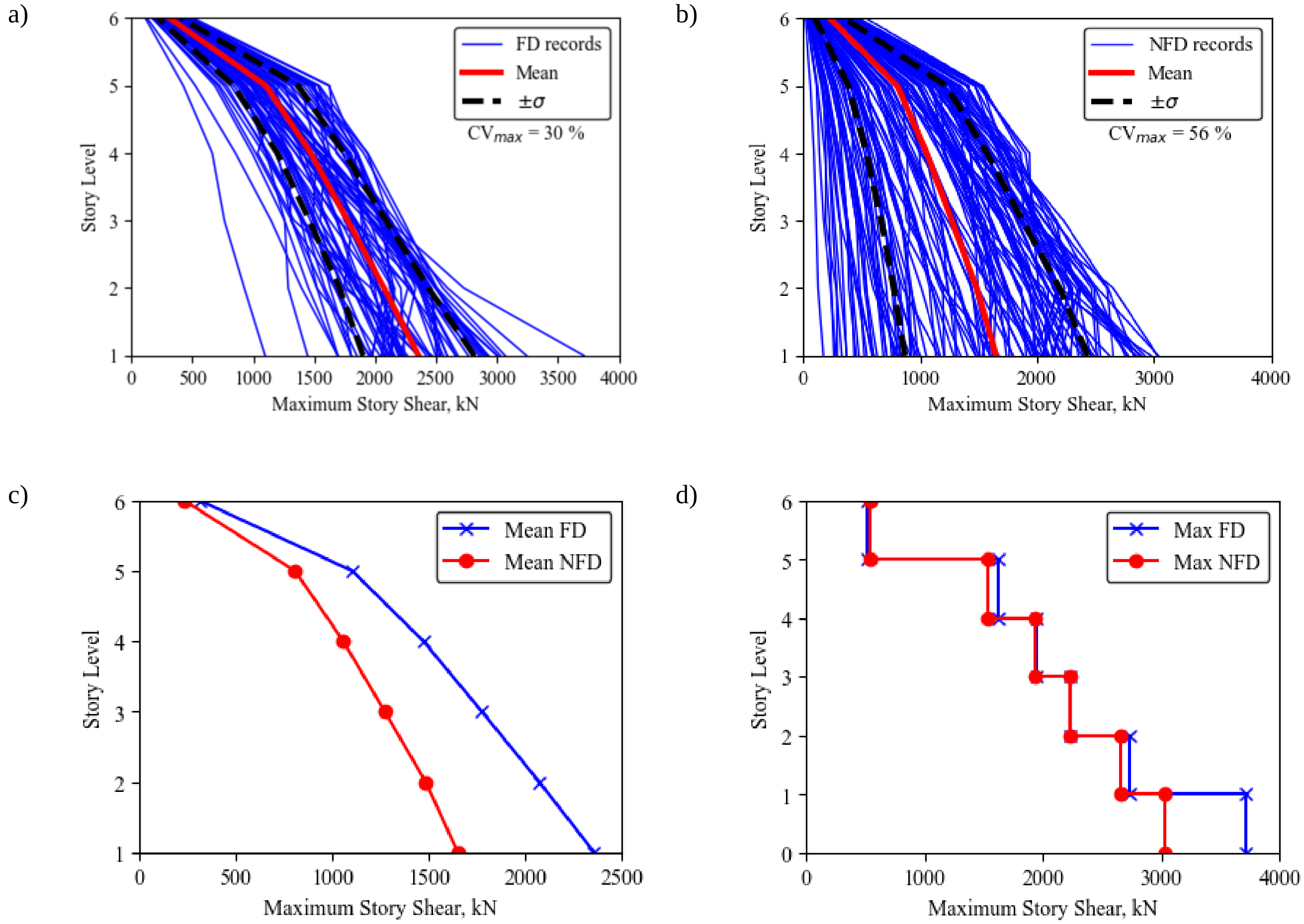


**Figure 10. The Maximum Story Shear (MSS) demand of MSB for: a) FD set, b) NFD set, c) Mean MSS demand of the FD and NFD sets, and d) Height-wise distribution of MSS demand.**

### *5.5 Optimal EDP-IM pairs of MSB*

By using the probabilistic seismic demand model framework, the optimality of IM-EDP pairs can be investigated[57]; however, the correlation criterion ($R^2$) is a statistical measure of how well the data match the fitted regression line. This criterion ranges from 0 to 1. In general, an EDP-IM correlation relationship with a high $R^2$ indicates less scattering. Figure 11 illustrates the variation of seismic peak responses with respect to earthquake intensity measures (Ims). In order to follow the trend of the responses, the near-field records are separately fitted with a quadratic curve [58], [59]. The figure illustrates how the near-field ground motions affect the seismic response of the MSB. The examined EDPs under the action of near-field ground motions are plotted in Figure 11 in terms of PGA, PGV, and $Sa(T_1,5_{\%})$, and the computed value of $R^2$ is separately listed in Table 3. Comparing the $R^2$ value of EDP-IM pairs show that forward directivity records have lower $R^2$ values than non-forward directivity records, indicating the presence of pulse causes scattering in the seismic response of the mid-rise MSB. Considering IDR and DR as EDP indicates that the high value of $R^2$ for Sa ($T_1$, 5%) compared to those for other IMs indicates that Sa ($T_1$, 5%) is a suitable predictor of structural response for forward-directivity and non-forward directivity earthquake ground motions. For EDP=MCA, PGA is the optimal IM for the prediction of MSB. However, IM=PGV is a poor predictor of MSB' EDPs under FD records. In general, Sa($T_1$, 5%) is recommended as an appropriate IM.

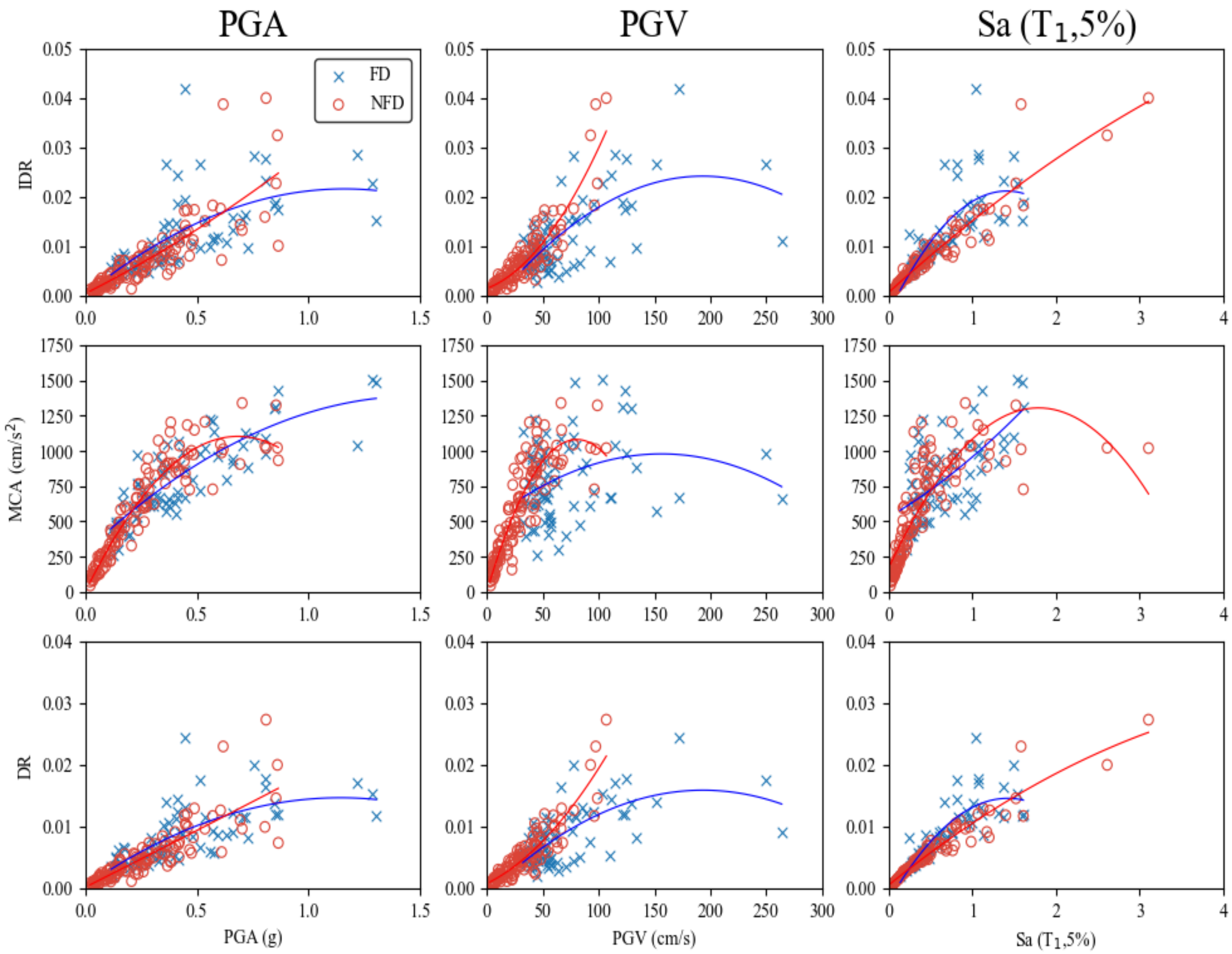


**Figure 11. IM-EDP curves for different earthquake parameters and seismic responses.**

**Table 3. A comparison of R2 values for the quadratic trend lines for different pairs of IM-EDP.**

| IM | PGA | | PGV | | Sa ($T_1$, 5%) | |
|---|---|---|---|---|---|---|
| **Ground motion** | FD | NFD | FD | NFD | FD | NFD |
| **IDR** | 0.59 | 0.85 | 0.46 | 0.84 | 0.76 | 0.96 |
| **MCA** | 0.72 | 0.91 | 0.09 | 0.86 | 0.42 | 0.84 |
| **DR** | 0.61 | 0.87 | 0.46 | 0.86 | 0.83 | 0.98 |

## 7. Investigation of equivalent pulses

A comparison of seismic responses of mid-rise MSBs subjected to FD ground motions and their equivalent pulses is presented in this section to assess how pulse presence may influence the seismic response of MSBs subjected to FD ground motions. Figure 12 illustrates the mean values of the EDPs along the MSB height. The peak responses under the actual FD records are considerably lower than those under the equivalent pulses. This indicates that near-field ground motions induce a greater seismic response for MSB than equivalent pulse ground motions. It also demonstrates that taking Baker's procedure into account, Equivalent pulses are incapable of reproducing the seismic demands of MSBs.

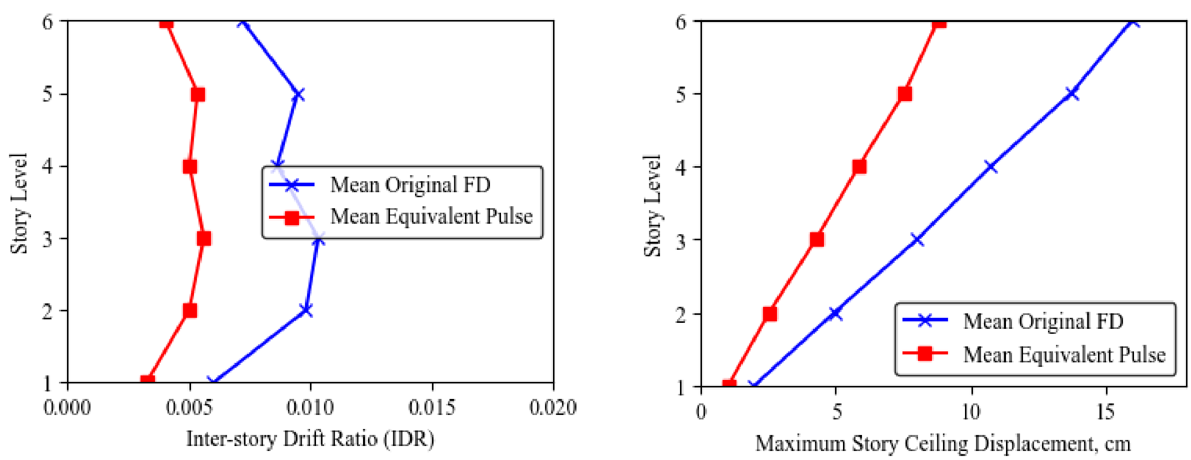

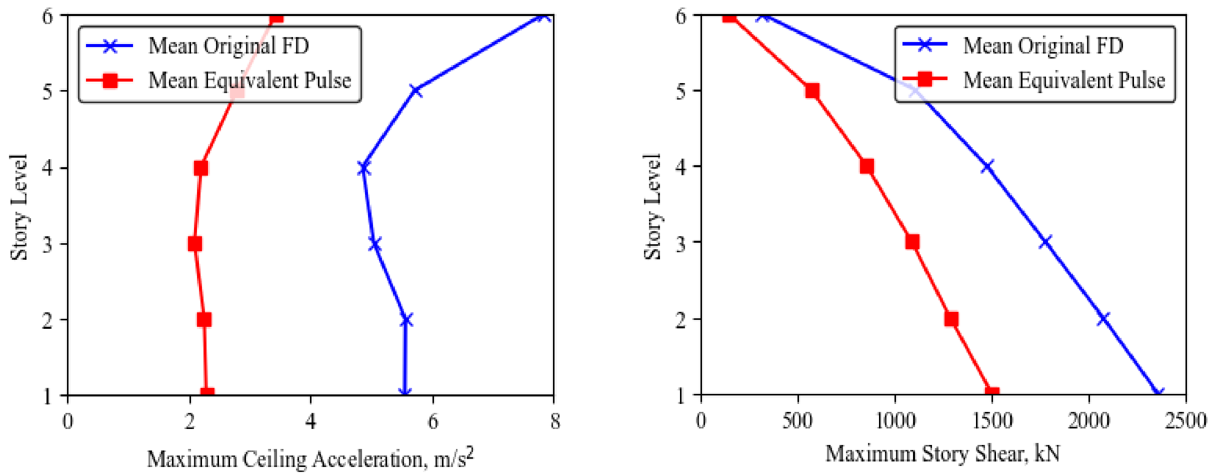


**Figure 12. Mean value of the seismic response of MSB under the main FD records and their equivalent pulses**

Seismic response analysis of the MSB under the action of equivalent pulse ground motions is illustrated in Figure 13, which provides an understanding of how the MSB performs under the action of equivalent pulse ground motions. As shown in this figure, the maximum coefficient of variation of the responses ($CV_{max}$) along the MSB height indicates that pulse records generate more scattering compared to FD records for all of the shown EDPs. Thus, the pulse nature of FD records seems to play an essential role in the dispersion of structural responses of the MSB.

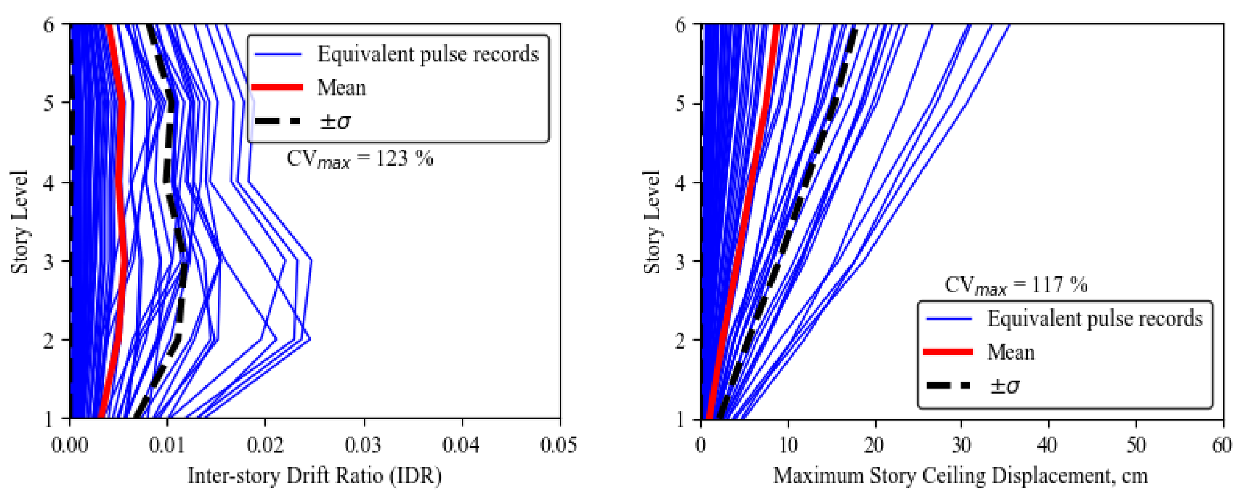

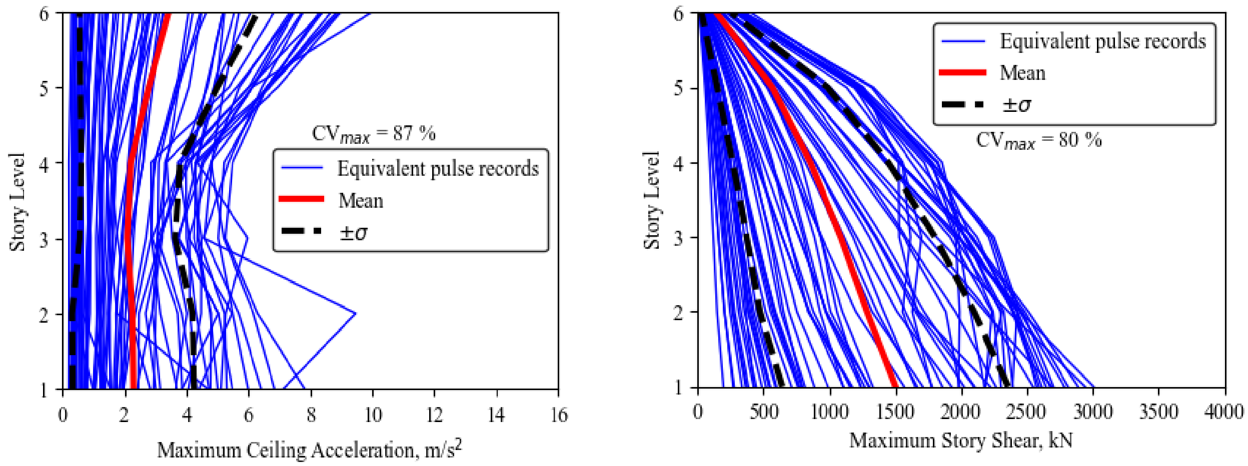


**Figure 13. Seismic response of the mid-rise MSB subjected to equivalent pulse ground motions**

For a more detailed investigation of the effect of equivalent pulse on mid-rise MSB, the following equation is used [41]:

$$\Psi(T,T_P) = \frac{EDP_{ep}(T,T_P)}{EDP_{ae}(T,T_P)} \tag{1}$$

Dominant pulse period is expressed by $T_p$, while a natural period is expressed by $T_1$=0.84s, and equivalent pulses are expressed by ep, and actual earthquakes by ae.

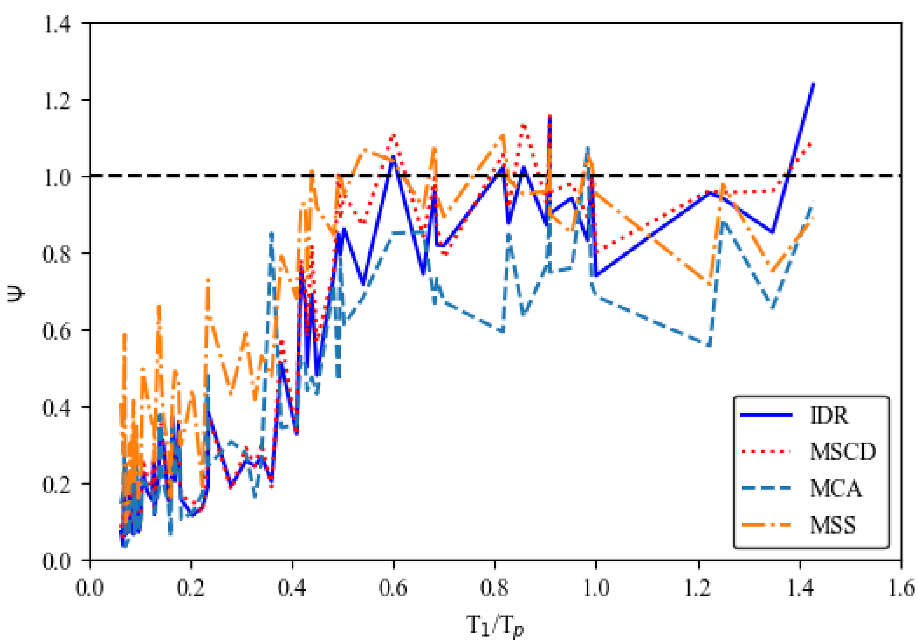


**Figure 14. Variation of the response ratio for different EDPs with respect to $T_1/T_p$.**

Figure 14 shows that while results obtained under equivalent pulses are more similar to those obtained under actual FD ground motions as $T_1/T_p$ increases, the characteristics of the near-fault records are typically not captured by the equivalent pulses when compared to the actual FD records. This is due to Baker's method's focus on the velocity pulse alone; as a result, it is unable to reproduce the frequency content of the main FD earthquake ground motions beyond of those that are connected to the velocity pulse [60]. However, at some points, the distinctive features of the velocity pulse have caused $\psi>1$. Interestingly, 20% of the equivalent pulses produced by the FD records in $0.7 < T_1/T_{P,\ Baker} < 1$ range for all EDPs other than MCA were proven to be capable of anticipating the seismic demands of the MSB. Therefore, under these conditions, strong pulses govern structural responses, or the equivalent pulse from the original FD records is capable of reproducing the original records' results.

It is possible to conduct an in-depth analysis of the acceleration and velocity response spectra of the FD records and their corresponding pulses in order to gain a deeper comprehension of the reasons behind why the forward-directivity pulse controls structural response when $0.7< T_1/T_{P,\ Baker} <1$. In order to do this, three records with $T_1/T_p$ values of 0.90, 0.54, and 0.17 have been shown in Figure 15 to explore the response spectra of these values. Their corresponding mean value of $\psi$ are 1.07, 0.83 and 0.37, respectively.

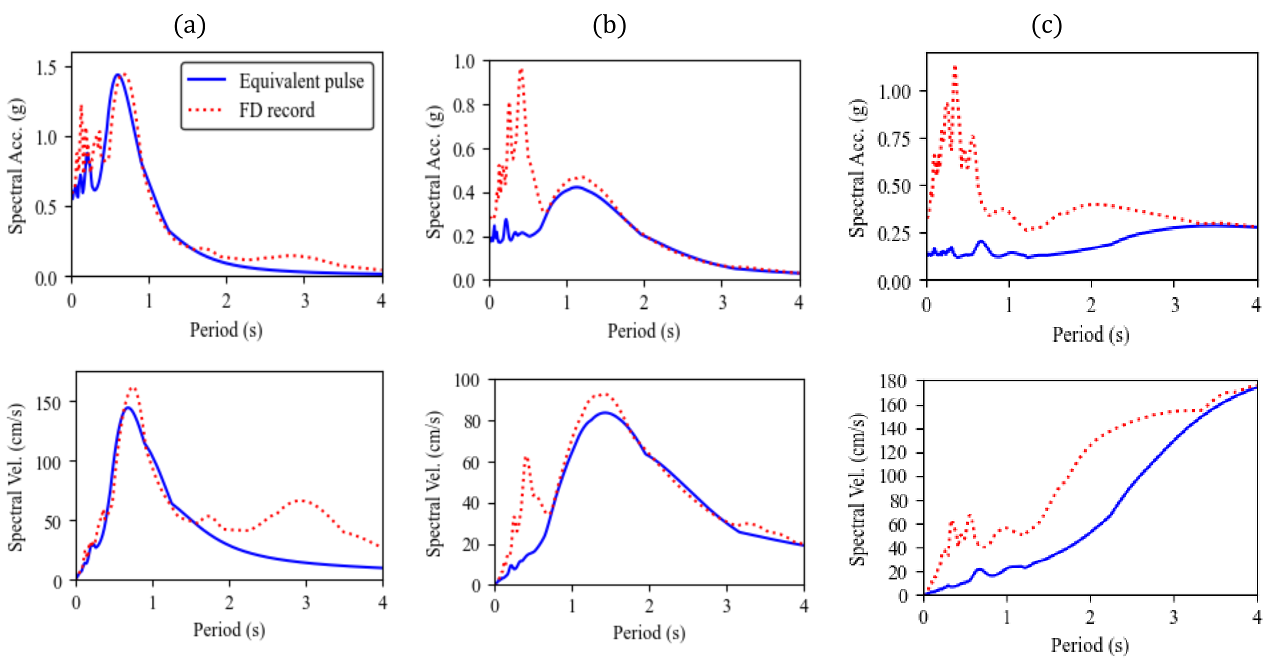


**Figure 15. The acceleration and velocity response spectra of actual FD records and their corresponding equivalent pulses when T1/Tp is: (a) 0.90, (b) 0.57, and (c) 0.17**

In this figure, it can be seen that the extracted pulses and the recorded ground motions have peaks at approximately the same spectral period, which is near the fundamental structural period. Decreasing the period ratio reduces the similarity between the velocity response spectra of the equivalent pulses and the FD ground motions, resulting in a very different response spectrum for equivalent pulses. Moreover, other peaks have been observed in the response spectrum of the FD ground motions near the natural mode periods that govern the behavior of the mid-rise MSB. In order to represent FD ground motions using simplified pulses, these peaks are filtered out [41]. According to Figure 15(c), the equivalent pulse has a period that is too long to excite the MSB. The equivalent pulse will therefore be unable to adequately reproduce the frequency content and spectral values of the actual FD record below the proposed period range. This is especially true in the vicinity of natural frequencies of the MSB.

Figure 16 and Figure ***17*** show IDR distributions for FD ground motions and equivalent pulses over the height of the mid-rise MSB for three ranges of pulse parameters, including pulse period (Tp) and pulse amplitude (Ap). Depending on the pulse period of the earthquake, the amplitude deviation of the seismic response across the height of the MSB is negligible when Tp is long (Tp>6s). When the pulse period decreases, however, the difference immediately increases. Moreover, in the case of low pulse amplitudes, the amplitude deviation of the seismic response over the MSB height may be overlooked. In spite of this, as the pulse amplitude increases, the difference increases rapidly. A similar trend was observed for other EDPs as well.

IDR distributions change based on pulse parameter values. When the pulse period increases, the IDR shifts from the lower to higher stories of the structure. In contrast, when the pulse's amplitude increases, the IDR moves from the structure's upper levels to its lower levels.

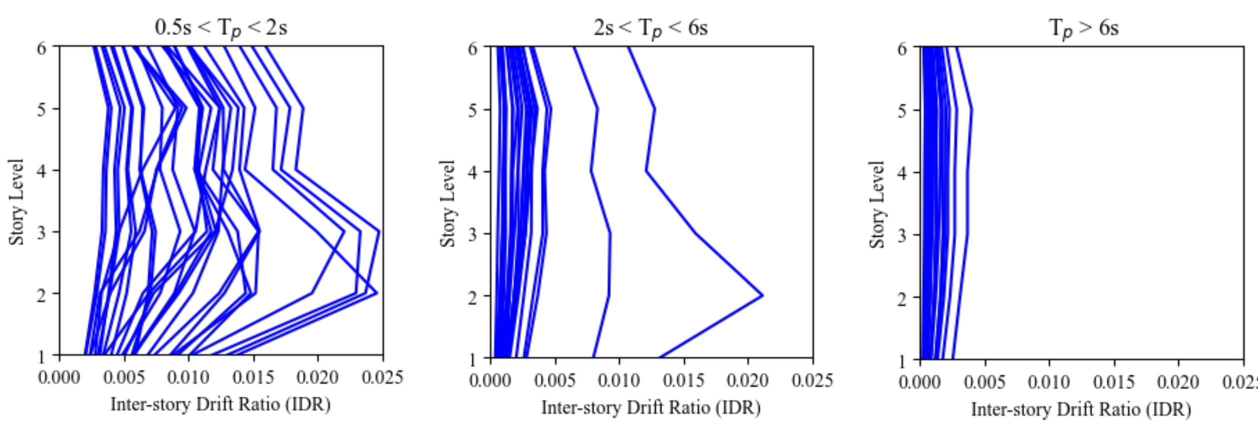


**Figure 16. Inter-story drift ratio along the MSB height under the equivalent pulses for various pulse periods**

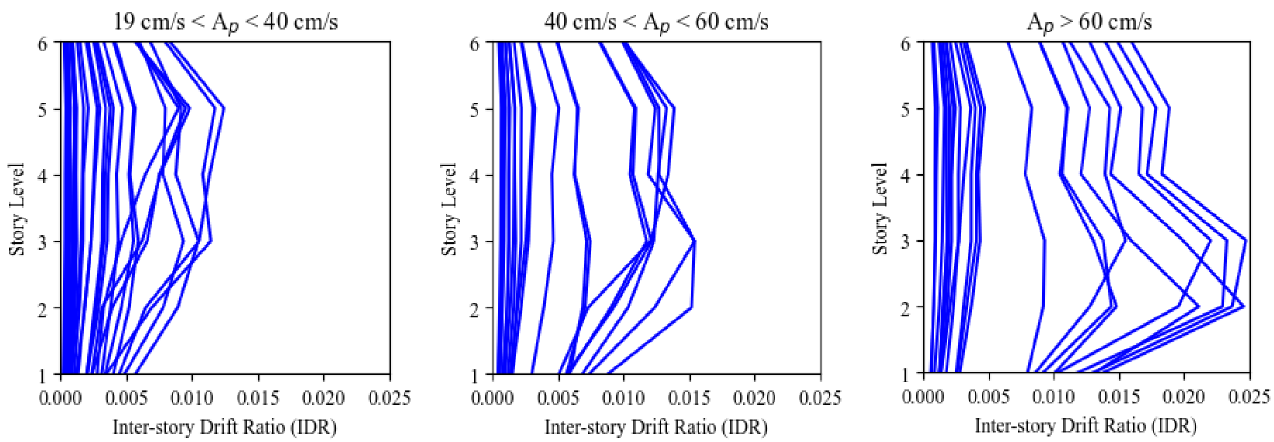


**Figure 17. Inter-story drift ratio along the MSB height under the equivalent pulses for various pulse amplitudes**

Figure 18 illustrates the influence of pulse period and pulse amplitude parameters on the nonlinear seismic response of the MSB by illustrating the inter-story drift and displacement in the MSB in response to FD records. According to this figure, increasing the dominant pulse's amplitude causes IDR and displacement to increase, while increasing the pulse period causes them to decrease.

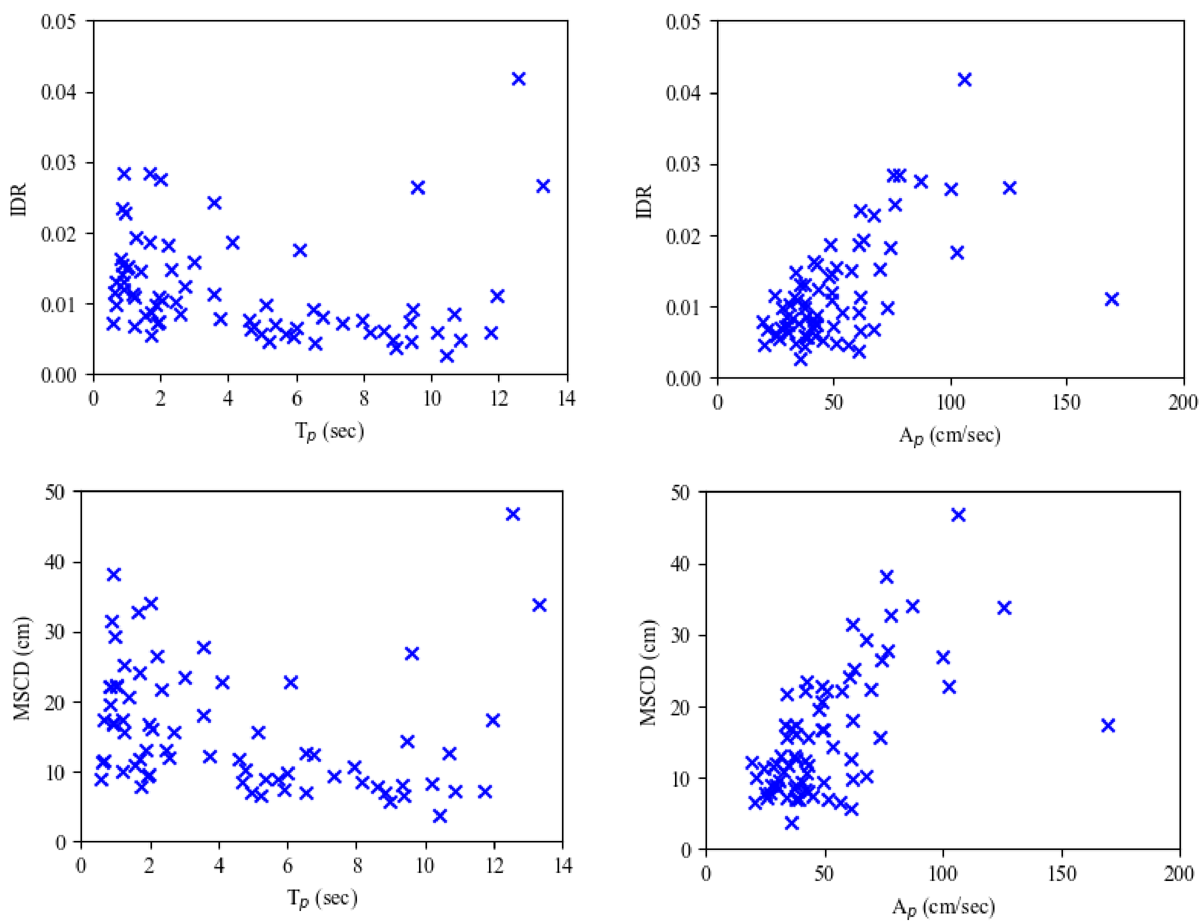


**Figure 18. Comparing IDR and MSCD under the action of FD records with dominant velocity pulse parameters.**

## 8. Concluding remarks

Identifying the seismic behavior of MSB subjected to near-field ground motions is an essential issue for engineers and researchers to accommodate seismic design codes. The main focus of this study is to assess the nonlinear seismic responses of MSB undergoing near-field earthquakes and whether the corresponding pulses can predict the structural response to the original forward-directivity ground motions. For this purpose, the nonlinear seismic response of the mid-rise Modular Steel Building was examined under the action of 72 near-field earthquake records with forward-directivity effect and 120 ordinary near-field earthquake records. Baker's method was used to examine and extract the pulses in the forward-directivity near-field earthquake ground motions. In addition, it was also investigated how the pulse characteristics affected the seismic response of the MSB. The primary results showed that degradation of stiffness and strength of mid-rise MSB under forward-directivity ground motions are more evident and structure is more prone to damage, and this is due to the initial velocity pulse of the FD records. Inter-connections were also modeled to connect the modules: (1) vertical inter-connection using a zero-length element with axial, shear, and moment behavior, and (2) horizontal inter-connection using a link element with axial, shear, and moment behavior. The main findings of the study can be summarized as follows:

- Due to the IDR demands concentrating at the intermediate story levels, the intermediate parts of mid-rise MSBs are more vulnerable to damage than the upper and lower stories when affected by both FD and NFD ground motions.

- According to a comparison of the displacement response of the mid-rise MSB under forward-directivity and non-forward-directivity records, forward-directivity records have a displacement response approximately twice as great as non-forward-directivity records. FD records have a higher PGV than NFD records, which might explain the difference.

- It was observed that the mean and maximum values of the maximum story shear responses for MSB under the FD records are both higher than under the NFD records in terms of mean and maximum values.

- Among the investigated intensity measures in the FD records, Sa (T1, 5%) exhibits a good correlation with EDPs. In the NFD records, all considered IMs and EDPs are correlated well. In contrast, the relationship between Sa (T1, 5%) and structural response appears to be stronger. Therefore, it can be concluded that the destructive power of near-field earthquake ground motions is proportional to their Sa (T1, 5%) records, with the higher the Sa (T1, 5%) record, the greater the impact on the mid-rise MSB.

- When the equivalent pulse is compared with the actual FD records, the equivalent pulses tend to predict the seismic demands of the MSB less than the actual FD records, especially as the pulse period increases. However, the equivalent pulse response can be equal to FD responses or even greater for 0.7 < T1/Tp, Baker< 1.
- It was observed that as the pulse period increases and pulse amplitude decreases, the amplitude deviation of seismic response across the MSB's height becomes smoother. The opposite trend was seen by a decrease in the pulse period and an increase in pulse amplitude.

## References


[1] Y. S. Chua, J. Y. R. Liew, and S. D. Pang, "Modelling of connections and lateral behavior of high-rise modular steel buildings," *J. Constr. Steel Res.*, vol. 166, p. 105901, 2020.

[2] M. Alembagheri, P. Sharafi, M. Rashidi, A. Bigdeli, and M. Farajian, "Natural dynamic characteristics of volumetric steel modules with gypsum sheathed LSF walls: Experimental study," in *Structures*, 2021, vol. 33, pp. 272–282.

[3] P. Sharafi, M. Rashidi, M. Alembagheri, and A. Bigdeli, "System Identification of a Volumetric Steel Modular Frame Using Experimental and Numerical Vibration Analysis," *J. Archit. Eng.*, vol. 27, no. 4, p. 04021032, 2021.

[4] M. Alembagheri, P. Sharafi, R. Hajirezaei, and Z. Tao, "Anti-collapse resistance mechanisms in corner-supported modular steel buildings," *J. Constr. Steel Res.*, vol. 170, p. 106083, 2020.

[5] Z. Chen, J. Liu, Y. Yu, C. Zhou, and R. Yan, "Experimental study of an innovative modular steel building connection," *J. Constr. Steel Res.*, vol. 139, pp. 69–82, 2017.

[6] T. Munmulla *et al.*, "Analyses of Structural Robustness of Prefabricated Modular Buildings: A Case Study on Mid-Rise Building Configurations," *Buildings*, vol. 12, no. 8, p. 1289, 2022.

[7] C. D. Annan, M. A. Youssef, and M. H. El Naggar, "Seismic vulnerability assessment of modular steel buildings," *J. Earthq. Eng.*, vol. 13, no. 8, pp. 1065–1088, 2009.

[8] C. D. Annan, M. A. Youssef, and M. H. El Naggar, "Seismic overstrength in braced frames of modular steel buildings," *J. Earthq. Eng.*, vol. 13, no. 1, pp. 1–21, 2008.

[9] Z. Wang and K. D. Tsavdaridis, "Optimality criteria-based minimum-weight design method for modular building systems subjected to generalised stiffness constraints: A comparative study," *Eng. Struct.*, vol. 251, p. 113472, 2022.

[10] J. P. Singh, “Earthquake ground motions: implications for designing structures and reconciling structural damage,” *Earthq. spectra*, vol. 1, no. 2, pp. 239–270, 1985.

[11] P. G. Somerville, N. F. Smith, R. W. Graves, and N. A. Abrahamson, “Modification of empirical strong ground motion attenuation relations to include the amplitude and duration effects of rupture directivity,” *Seismol. Res. Lett.*, vol. 68, no. 1, pp. 199–222, 1997.

[12] G. P. Mavroeidis and A. S. Papageorgiou, “A mathematical representation of near-fault ground motions,” *Bull. Seismol. Soc. Am.*, vol. 93, no. 3, pp. 1099–1131, 2003.

[13] A. K. Agrawal and W. L. He, “A close-form approximation of near-fault ground motion pulses for flexible structures,” 2002.

[14] J. W. Baker, “Quantitative classification of near-fault ground motions using wavelet analysis,” *Bull. Seismol. Soc. Am.*, vol. 97, no. 5, pp. 1486–1501, 2007.

[15] N. Makris, “Rigidity--plasticity--viscosity: Can electrorheological dampers protect base-isolated structures from near-source ground motions?,” *Earthq. Eng. Struct. Dyn.*, vol. 26, no. 5, pp. 571–591, 1997.

[16] M. Sasani and V. V Bertero, “Importance of Severe Pulse-Type Ground Motions in Performance-Based Engineering: Historical and Critical,” in *Proceedings of the 12th World Conference on Earthquake Engineering, New Zealand Society for Earthquake Engineering, Upper Hutt, New Zealand*, 2000.

[17] B. Alavi and H. Krawinkler, “Consideration of near-fault ground motion effects in seismic design,” in *Proceedings of the 12th World Conference on Earthquake Engineering*, 2000, vol. 8, p. 2000.

[18] J. D. Bray and A. Rodriguez-Marek, “Characterization of forward-directivity ground motions in the near-fault region,” *Soil Dyn. Earthq. Eng.*, vol. 24, no. 11, pp. 815–828, 2004.

[19] J. C. Anderson and V. V Bertero, “Uncertainties in establishing design earthquakes,” *J. Struct. Eng.*, vol. 113, no. 8, pp. 1709–1724, 1987.

[20] J. F. Hall, T. H. Heaton, M. W. Halling, and D. J. Wald, “Near-source ground motion and its effects on flexible buildings,” *Earthq. spectra*, vol. 11, no. 4, pp. 569–605, 1995.

[21] H. Krawinkler and B. Alavi, “Development of improved design procedures for near-fault ground motions,” in *SMIP98 Seminar on Utilization of Strong-Motion Data*, 1998, vol. 15.

[22] G. Mylonakis and A. M. Reinhorn, “Yielding oscillator under triangular ground acceleration pulse,” *J. Earthq. Eng.*, vol. 5, no. 02, pp. 225–251, 2001.

[23] Y. Zhang and W. D. Iwan, “Active interaction control of tall buildings subjected to near-field ground motions,” *J. Struct. Eng.*, vol. 128, no. 1, pp. 69–79, 2002.

[24] Y. Yazdani and M. Alembagheri, “Effects of base and lift joints on the dynamic response of concrete gravity dams to pulse-like excitations,” *J. Earthq. Eng.*, vol. 21, no. 5, pp. 840–860, 2017.

[25] B. Alavi and H. Krawinkler, “Behavior of moment-resisting frame structures subjected to near-fault ground motions,” *Earthq. Eng. Struct. Dyn.*, vol. 33, no. 6, pp. 687–706, 2004.

[26] G. P. Mavroeidis, G. Dong, and A. S. Papageorgiou, “Near-fault ground motions, and the response of elastic and inelastic single-degree-of-freedom (SDOF) systems,” *Earthq. Eng. Struct. Dyn.*, vol. 33, no. 9, pp. 1023–1049, 2004.

[27] E. Kalkan and S. K. Kunnath, "Effects of fling step and forward directivity on seismic response of buildings," *Earthq. Spectra*, vol. 22, no. 2, pp. 367–390, 2006.

[28] M. Alembagheri, P. Sharafi, Z. Tao, R. Hajirezaei, and K. Kildashti, "Robustness of multistory corner-supported modular steel frames against progressive collapse," *Struct. Des. Tall Spec. Build.*, vol. 30, no. 18, p. e1896, 2021.

[29] L. Fiorino, V. Macillo, and R. Landolfo, "Shake table tests of a full-scale two-story sheathing-braced cold-formed steel building," *Eng. Struct.*, vol. 151, pp. 633–647, 2017.

[30] V. Macillo, L. Fiorino, and R. Landolfo, "Seismic response of CFS shear walls sheathed with nailed gypsum panels: Experimental tests," *Thin-Walled Struct.*, vol. 120, pp. 161–171, 2017.

[31] A. Fathieh and O. Mercan, "Seismic evaluation of modular steel buildings," *Eng. Struct.*, vol. 122, pp. 83–92, 2016.

[32] Y. Hu, L. Jiang, J. Ye, X. Zhang, and L. Jiang, "Seismic responses and damage assessment of a mid-rise cold-formed steel building under far-fault and near-fault ground motions," *Thin-Walled Struct.*, vol. 163, p. 107690, 2021.

[33] V. V Bertero, S. A. Mahin, and R. A. Herrera, "Aseismic design implications of near-fault San Fernando earthquake records," *Earthq. Eng. Struct. Dyn.*, vol. 6, no. 1, pp. 31–42, 1978.

[34] V. Sharma, M. K. Shrimali, S. D. Bharti, and T. K. Datta, "Seismic fragility evaluation of semi-rigid frames subjected to near-field earthquakes," *J. Constr. Steel Res.*, vol. 176, p. 106384, 2021.

[35] W.-I. Liao, C.-H. Loh, and S. Wan, "Earthquake responses of RC moment frames subjected to near-fault ground motions," *Struct. Des. Tall Build.*, vol. 10, no. 3, pp. 219–229, 2001.

[36] R. Sehhati, A. Rodriguez-Marek, M. ElGawady, and W. F. Cofer, "Effects of near-fault ground motions and equivalent pulses on multi-story structures," *Eng. Struct.*, vol. 33, no. 3, pp. 767–779, 2011.

[37] M. Gerami and D. Abdollahzadeh, "Vulnerability of steel moment-resisting frames under effects of forward directivity," *Struct. Des. Tall Spec. Build.*, vol. 24, no. 2, pp. 97–122, 2015.

[38] F. Taiyari, A. Formisano, and F. M. Mazzolani, "Seismic behaviour assessment of steel moment resisting frames under near-field earthquakes," *Int. J. Steel Struct.*, vol. 19, no. 5, pp. 1421–1430, 2019.

[39] I. Mansouri, S. Shahbazi, J. W. Hu, and S. A. Moghaddam, "Effects of pulse-like nature of forward directivity ground motions on the seismic behavior of steel moment frames," *Earthq. Struct*, vol. 17, no. 1, pp. 1–15, 2019.

[40] Q. Xu, S. Xu, J. Chen, and J. Li, "Dimensionless analysis of pulse-like effects on the seismic behavior of a dam based on wavelet-decomposed near-fault ground motions," in *Structures*, 2021, vol. 33, pp. 2003–2018.

[41] Y. Yazdani and M. Alembagheri, "Nonlinear seismic response of a gravity dam under near-fault ground motions and equivalent pulses," *Soil Dyn. Earthq. Eng.*, vol. 92, no. November 2016, pp. 621–632, 2017.

[42] P. Rajeev and S. Tesfamariam, "Seismic fragilities of non-ductile reinforced concrete frames with consideration of soil structure interaction," *Soil Dyn. Earthq. Eng.*, vol. 40, pp. 78–86, 2012.

[43] F. M. Nazri, C. G. Tan, and S. N. A. Saruddin, “Fragility curves of regular and irregular moment-resisting concrete and steel frames,” *Int. J. Civ. Eng.*, vol. 16, no. 8, pp. 917–927, 2018.

[44] S. J. Thachampuram, “Development of fragility curves for an RC frame,” 2014.

[45] H. Tajammolian, F. Khoshnoudian, A. R. Rad, and V. Loghman, “Seismic fragility assessment of asymmetric structures supported on TCFP bearings subjected to near-field earthquakes,” in *Structures*, 2018, vol. 13, pp. 66–78.

[46] H. Beiraghi, “Incremental dynamic analysis of coupled tall reinforced concrete walls subjected to far-field and near-field earthqu,” *Ing. Sismica*, vol. 37, no. 3, pp. 1–27, 2020.

[47] P. E. E. R. Center, “PEER strong motion database.” University of California, Berkeley Berkeley, CA, 2000.

[48] B. Alavi and H. Krawinkler, “Strengthening of moment-resisting frame structures against near-fault ground motion effects,” *Earthq. Eng. Struct. Dyn.*, vol. 33, no. 6, pp. 707–722, 2004.

[49] G. Wu, C. Zhai, S. Li, and L. Xie, “Effects of near-fault ground motions and equivalent pulses on Large Crossing Transmission Tower-line System,” *Eng. Struct.*, vol. 77, pp. 161–169, 2014.

[50] A. 360-10, “Specification for structural steel buildings,” *Am. Inst. Steel Constr.*, 2010.

[51] A. ANSI, “ANSI/AISC 360-10. Specification for structural steel buildings, American Institute of Steel Construction,” *Inc. Chicago*, 2010.

[52] P.-C. Hsiao, *Seismic performance evaluation of concentrically braced frames*. University of Washington, 2012.

[53] A. S. of Civil Engineers (ASCE), “ASCE/SEI 7-16: Minimum Design Loads for Buildings and Other Structures,” 2016.

[54] A. J. Styles, F. J. Luo, Y. Bai, and J. B. Murray-Parkes, “Effects of joint rotational stiffness on structural responses of multi-story modular buildings,” in *Transforming the Future of Infrastructure through Smarter Information: Proceedings of the International Conference on Smart Infrastructure and ConstructionConstruction, 27--29 June 2016*, 2016, pp. 457–462.

[55] D.-A. Corfar and K. D. Tsavdaridis, “A comprehensive review and classification of inter-module connections for hot-rolled steel modular building systems,” *J. Build. Eng.*, vol. 50, p. 104006, 2022.

[56] D.-A. Corfar and K. D. Tsavdaridis, “A Novel Optimised Inter-Locking Connection For Steel Modular Building Systems To Enable Re-Use,” 2022.

[57] H. Haghgou, M. Alembagheri, and A. Bigdeli, “Determination of optimal intensity measure for probabilistic seismic demand analysis of intake towers,” *Structures*, vol. 34, no. January, pp. 1998–2013, 2021.

[58] J. J. Bommer, J. Hancock, and J. E. Alarcón, “Correlations between duration and number of effective cycles of earthquake ground motion,” *Soil Dyn. Earthq. Eng.*, vol. 26, no. 1, pp. 1–13, 2006.

[59] A. Emami Koupaei, H. Saffari, and R. Rasti, “Investigating the Effect of Earthquake Duration on Concrete Structures by Analyzing the Frequency Content of Acceleration Time History,”

*J. Rehabil. Civ. Eng.*, vol. 9, no. 2, pp. 21–40, 2021.

[60] Q. Fu and C. Menun, “Seismic-environment-based simulation of near-fault ground motions,” in *Proceedings of the 13th world conference on earthquake engineering*, 2004.